TECHNISCHE UNIVERSITÄT MÜNCHEN

Institut für Röntgendiagnostik
(Direktor Univ.-Prof. Dr. E. J. Rummeny)

Visualization of Stem Cell Differentiation and Gene Expression Using a Galactosidase-Sensitive Contrast Agent for Magnetic Resonance Imaging

Daniel Matthew Golovko

Vollständiger Abdruck der von der Fakultät für Medizin der Technischen Universität München zur Erlangung des akademischen Grades eines

Doktors der Medizin

genehmigten Dissertation.

Vorsitzender:		Univ.-Prof. Dr. D. Neumeier
Prüfer der Dissertation:	1.	Priv.-Doz. Dr. H. E. Daldrup-Link (schriftliche Beurteilung)
		Univ.-Prof. Dr. E. J. Rummeny (mündliche Prüfung)
	2.	Univ.-Prof. Dr. J. G. Duyster

Die Dissertation wurde am 09.02.2009 bei der Technischen Universität München eingereicht und durch die Fakultät für Medizin am 16.12.2009 angenommen.

Table of Contents

Introduction

Therapeutic Approaches with Stem Cells

In order to understand therapeutic approaches based on stem cells, it is necessary to review a couple of definitions. Stem cells possess two important characteristics distinguishing them from other cell types. Firstly, they are undifferentiated cells that have the capacity to generate large number of progeny through cell division while retaining their multi-lineage potential [37]. Secondly, under certain physiological or experimental conditions, they can give rise to specialized cell types such as dopaminergic neurons, pancreatic β-cells or cardiomyocytes.

A stem cell's ability to differentiate into various cell types is described by its "potency." A fertilized egg is considered to be totipotent because it has the potential of generating all possible cells in an organism. This includes cells that are required for embryonic development, such as the placenta and extra-embryonic tissues. If a stem cell has the ability to create cells that originate from all three germ layers (mesoderm, endoderm and ectoderm), it is called pluripotent. Pluripotent stem cells give rise to the human body. They can be isolated from human embryos and some fetal tissue. Unipotent stem cells are usually found in adult organisms and are capable of differentiating along only one lineage. An overview can be found in Figure 1.

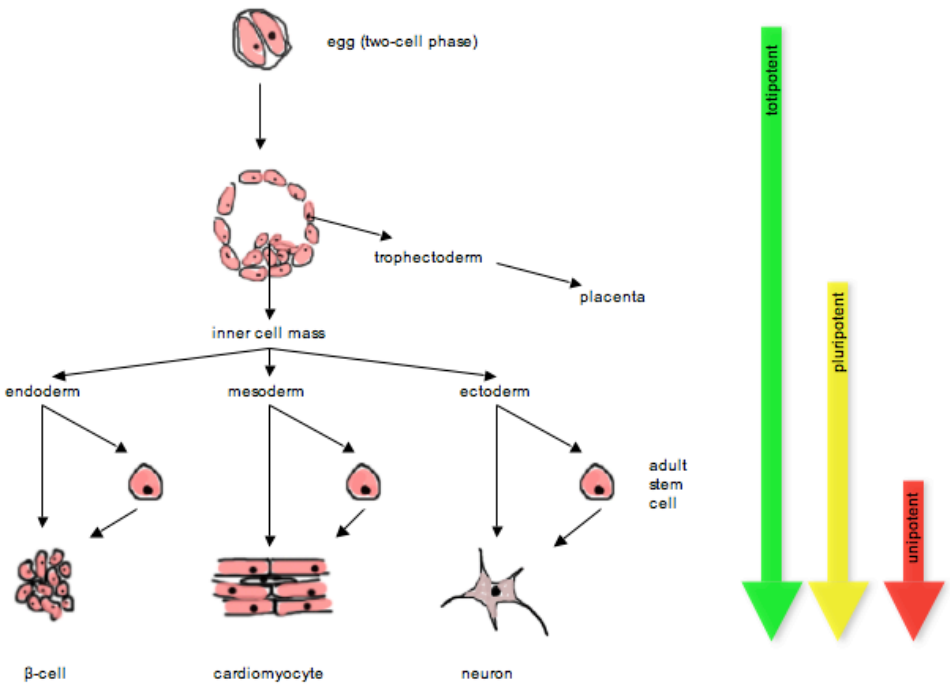

Figure 1 An overview of stem cell development.

Stem cells are further distinguished by their origin between embryonic and adult stem cells. There are three basic types of stem cells derived from the embryo – embryonic stem cells (ES), embryonic germ cells (EG) and embryonic carcinoma cells (EC) [82]. ES cells are derived from the inner cell mass of a blastocyst and were first isolated from human embryos by Thomson et al in 1998 [92]. EG cells can be collected from the primordial germ cells of the embryo or fetus. In normal development, EG cells are involved in developing the testes or ovaries and give rise to sperm or eggs. EC cells give rise to teratocarcinoma, an embryonic neoplasm containing tissue from at least two germ layers [96]. EC cells possess stem cell properties.

Adult stem cells are unspecialized cells that occur in specialized tissue. These cells exhibit neither the pluripotency of embryonic stem cells nor the indefinite capacity for replication, however they have been extensively studied and applied therapeutically [37]. This is the case with hematopoietic stem cells found in bone marrow that normally give rise to the plethora of cell types circulating in the blood. Under the correct conditions, these cells can differentiate to adipocytes, chondrocytes, skeletal muscle and other cell types [54]. One promising cell type is the multipotent

adult progenitor cell (MAPC) that Jiang et al characterized [45]. MAPCs were viable for more than 120 population doublings and were successfully differentiated to mesodermal endothelium, hepatocyte-like cells and neuronal lineages.

It was long thought that some organs, such as the brain and the heart, have no capacity for self-renewal. This has turned out to be false. Multipotent neural progenitor cells that are capable of forming neurons have been found in the human subcortical white matter [71]. Beltrami et al showed that the adult heart has a sub-population of myocytes that are not terminally differentiated and can undergo mitotic division after myocardial infarction [7]. While these adult stem cells are exceedingly rare in normal tissue, and cannot provide *restituio ad integrum*, they may play a role in future therapeutics.

As we have seen, there are many types of stem cells, accordingly, there are many different therapeutic approaches using stem cells. Perhaps the most invasive techniques involve extracting cells from a human embryo, differentiating and culturing these cells *ex vivo* with subsequent implantation into a patient. The "softer" end of the stem cell therapeutic spectrum strives to use pharmacological methods to mobilize endogenous stem cells in response to injury [36]. Classical therapeutic concepts usually require stem cells to differentiate and replace defective tissue, however studies have shown that stem cells, by their mere presence in injured tissue, can facilitate clinical improvements. It has been postulated that the mechanisms through which this occurs include the release of otherwise missing growth factors or transmitters that improve survival and function of damaged tissue [58]. In an animal model of amyotrophic lateral sclerosis (ALS, Lou Gehrig's disease), EG cells injected into the cerebral spinal fluid resulted in partial recovery of motor functions [47]. Analysis of the implanted cells made clear that neural differentiation of the EG cells could not have accounted for the functional recovery alone.

Most stem cell therapies aim to replace cells with little or no capacity of self-renewal that were lost through autoimmune, ischemic or degenerative processes. While this thesis focuses on applications in neurology, a quick discussion of type 1A diabetes mellitus and myocardial infarction is warranted because these are classical diseases for stem cell research. Transplantations of the pancreas and pancreatic islet

grafts pose successful therapeutic options for type 1A diabetes mellitus [91]. Pancreatic tissue derived from stem cells would alleviate the need for immunosuppression arising from the implantation of non-self material and solve the problem of the short supply of cadaveric donor organs. First reports of transplanted insulin-secreting ES cell clones reversing hyperglycemia in diabetic mice have been encouraging [88], however, scientists are still far from high volume production of pancreatic ß cells for transplantation.

Many investigators have described methods of stem cell derived myocardial regeneration. In mice models, ES-derived cardiomyocytes implanted into infarcted area improved heart functions [50]. Fetal cardiomyocytes can proliferate, mature, differentiate and integrate into host myocardium [87]. Bone marrow stem cell transplantation in humans by Strauer et al showed a positive effect on myocardial perfusion as well as function [90]. While myocardial regeneration is multi-faceted – for example, in addition to replacing cardiac tissue in the region of infarction, blood flow must be also renewed – these results paint a very promising picture for future therapies.

In 1995, Kleppner et al were successful in transplanting human neurons derived from a teratocarcinoma line into the brain of a mouse [49]. These cells matured, integrated and survived for over one year. Studies on humans based on this have shown therapeutic benefit. Teratoma cell lines implanted into patients after stroke improved outcomes using standardized quantification methods (European Stroke Scale) [52]. The same cell line resulted in motor evoked potentials and recovery of some motor function when implanted after spinal cord contusion in rats [84]. Other studies have shown that engrafted marked neuronal stem cells differentiate to neurons in the damaged hemisphere in animal models [75]. As with the animal model of ALS described previously, stem cells most likely improve function through multiple mechanisms, including, but not limited to neuronal differentiation.

Hope for patients with Parkinson's disease was aroused when transplantation of embryonic DA neurons into the putamen of affected patients resulted in successful integration of the cells and clinical improvement [31]. Another study, where fetal

nigral cells were transplanted, showed similar results [72]. Unfortunately, the implementation of these novel therapeutic approaches have not been as straightforward as one would have hoped for. In the fetal nigral transplantation for patients with Parkinson's disease, the outcome, while constituting a clinical improvement, was neither long-term nor applicable for the entire patient population, only providing improvement for patients less than 60 years old. In addition, many patients developed dyskinesias, making this form of therapy suboptimal for now. These studies show that stem cell biology is still in its infancy. Latest progress on stem cell research is indeed promising but at the same time elucidates the need for further studies. One of the many facets that require additional research concerns what happens to transplanted stem cells once they are in the body.

Imaging Methods to Visualize Homing and Engraftment of Transplanted Stem Cells

Usually, the method of delivery will involve injection of the stem cells systemically (into the blood system), into a cavity (into a brain ventricle) or into tissue (into myocardium). But what happens to the cells once they are in the body? Do the stem cells actually end up where they are desired (homing)? Do they integrate themselves with the host tissue (engraftment)? These questions are of great importance when deriving stem cell based therapy.

There are various classical methods of showing distribution of stem cells in the body. Most rely on introducing a marker into the graft material that can be specifically stained after explantation. One common method that we will also be using in our experiments is the transfection of stem cells with a plasmid containing *lacZ*. *lacZ* encodes β-galactosidase, an enzyme not normally found in human cells. After explantation, fixation and staining of material to be examined (which will be described in greater detail), marked cells will stain while unmarked cells will not. The major drawback of this method is that sacrificing the test animal is necessary.

It would obviously be beneficial to image stem cells in vivo rather than ex vivo. This can be achieved using various strategies:

- Ex vivo labeling of the stem cell with a contrast agent prior to implantation
- Utilizing a transporter uniquely located on the stem cell to mediate contrast agent uptake after systemic injection
- Genetically varying the stem cell to express a substance that is active as a contrast agent

There are various approaches in the fields of nuclear and optical imaging that deserve mention before continuing with methods in MR imaging. Nuclear imaging approaches, which include scintigraphy, single photon emission computed tomography (SPECT) and positron emission tomography (PET), have high sensitivity but expose patients to radiation and image very little anatomic detail [42]. Direct labeling of stem cells is problematic because of introduction of ionizing radiation. Systemic injection of contrast agent with subsequent concentration in a specific cell population is possible. Mesenchymal stem cells transplanted into the spinal cord of rabbits were successfully visualized using ^{131}I-labeled transferrin injected into cerebrospinal fluid [24]. Mesenchymal stem cells express a higher level of transferrin receptors than surrounding cells and as a result concentrate radiolabeled transferrin. This resulted in increased tracer uptake that was demonstrated by scintigraphy.

Optical imaging uses the principles of bioluminescence or fluorescence to display images. Bioluminescence uses light generating enzymes (usually luciferase) to generate an image; fluorescence uses photons emitted after excitement by a laser. Optical imaging is very specific but can only image limited depths. Tolar et al used a transposon-based vector to introduce luciferase into the genome of MAPCs [93]. The resulting cells glowed in the dark! Homing and engraftment of bone marrow cells labeled with PKH, a non-specific fluorescent cell labeling method, was successfully measured through using a bone window in mice [6]. Optical imaging is a new, promising technology, and will definitely have applications in research and endoscopy, however, its surface oriented nature poses great limitations on its general usage.

In MR imaging, there are two basic modes – T_1-weighted and T_2-weighted imaging. Correspondingly we have contrast agents that have a predominately T_1 effect and contrast agents that have a predominately T_2 effect [80]. T_2 contrast agents* are typically superparamagnetic iron oxide (SPIO) particles. Superparamagnetic particles differentiate themselves from ferromagnetic particles by their smaller size and abscence of permanent magnetism. When introduced into tissue, they produce local magnetic field gradients when imaged using MR. These gradients disrupt the homogeneity of the magnetic field and thus reduce primarily the T_2^* and T_2 times. This results in hypointensities (decrease in signal intensity, darker color in the image) in tissue containing SPIO particles on the T_2^* and T_2-weighted MR image.

An interesting approach by Genove et al was to use an adenovirus vector encoding a metalloprotein from the ferritin family as an MR reporter [34]. Ferritin is used by cells to store iron intracellularly. The expressed ferritin caused enhanced Fe uptake and became superparamagnetic. Although the group only investigated injection of the vector directly into the brain of mice, this method could be used to label and subsequently visualize implanted stem cells.

Hematopoietic progenitor cells derived from umbilical cord blood were incubated with SPIO particles [20]. Test tubes containing these cells were imaged and displayed a significant decrease in signal intensity (Figure 2). The same type of labeling was used in a more recent study where 3×10^7 marked cells were intravenously injected into a mouse and then imaged [19]. The cells migrated from the blood stream into the bone marrow, spleen and liver. In these organs, a darkening of MR images was observed. This proves that it is possible to track homing of labeled stem cells in vivo using MR imaging.

* That is, contrast agents that have stronger T_2 versus T_1 effects.

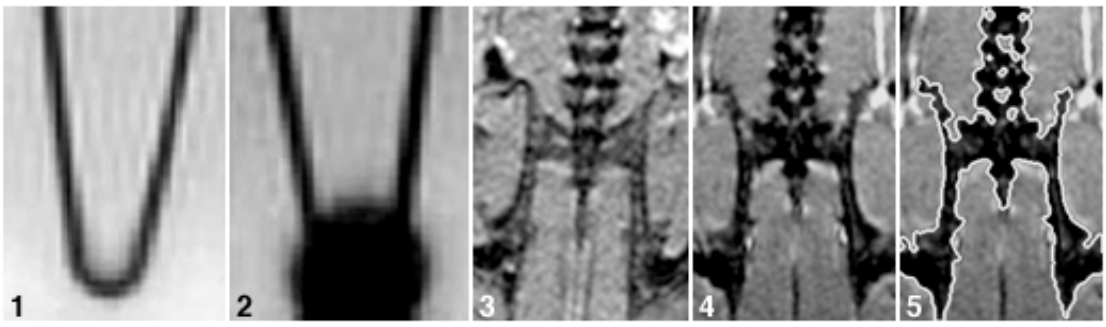

Figure 2 SPIO-labeled hematopoietic progenitor cells (1) non-labeled control cells (2) labeled cells showing strong T_2^* effect (3) coronal MRI of a mouse sacrum before injection with labeled cells (4) 24h after injection of labeled cells shows decreased signal intensity in bone marrow (5) outline of the mouse sacrum for orientation. (1) and (2) are T_2^*-weighted, (3) and (4) are T_2-weighted. From **[20, 21]**.

There have been many other studies using stem cells labeled with T_2 contrast agents, including endothelial precursor cells [3], mesenchymal stem cells [4] and ES cells [39]. One drawback of iron oxide labeling is that over time, a decrease in contrast effect can be noted [20]. This is probably because of degradation of the contrast agent coating and subsequent metabolism of the iron oxide particles. In addition, given the nature of T_2 imaging, magnetic field inhomogeneities due to metallic implants (such as shunts) or hemosiderin deposits after hemorrhage could be mistaken for the magnetic field inhomogeneities due to SPIO contrast.

Stem cells labeled with the typical T_1 contrast agent gadolinium (Gd) show no such signs. T_1 contrast agents are metal ions with unpaired electrons in their centers that, upon interaction with protons, shorten T_1 relaxation times [80]. A shorter T_1 time leads to spins recovering faster which leads to higher signal. Tissue containing Gd based agents therefore show up hyperintense (brighter color in the image) in T_1-weighted images.

Endothelial progenitor cells were successfully labeled when incubated with Gd-based contrast agent [16]. The contrast agent used was actually a dual agent with MR (caused by Gd) and optical imaging (caused by fluorescence) properties. When injected under the kidney capsule of mice, labeled cells were visible both through MR imaging in vivo as well as fluorescent microscopy after explantation. Another dual

agent, gadophorin-2, a fluorescent molecule that complexes Gd, was used to label mononuclear peripheral blood cells [18]. After injection into mice, the cells accumulated in the liver, spleen and bone marrow. This homing of cells was proven by in vivo MR imaging, in vivo and ex vivo optical imaging and ex vivo fluorescent microscopy.

Modo et al utilized a Gd rhodamine dextran (another dual agent) to label embryonic hippocampal cells [67]. Approximately 10^5 cells were then injected into the hippocampus of mice after induced global cerebral ischemia. Ex vivo MR imaging showed increased signal around the injection tract and corpus callosum, which suggests cell migration into the corpus callosum. These results corresponded to findings after fluorescent microscopy of the same tissue. An important consideration for labeling in general is that utilized contrast agent should be neither toxic to the cell nor harmful to its ability to differentiate. Here, Gd rhodamine dextran labeled cells showed good viability and successful differentiation to astrocytes and neurons, which was proven after histological analysis. While detrimental effects on viability and differentiation cannot be excluded, most contrast agents introduced here show no such signs.

One disadvantage of Gd based contrast agents are their relatively low sensitivity when compared to iron oxide agents [29]. To achieve detection levels comparable to iron oxides, one must achieve fairly high intracellular Gd concentrations. Because simple incubation of cells with Gd will not provide a detectable amount inside the cell, various transfection methods have been developed. One method involves specific peptide sequences that allow the protein carrying those sequences to become internalized. These sequences are known as membrane translocation signals. One such signal is the HIV Tat protein. A Gd chelate bound to a Tat-derived protein was successfully used to label cells [8]. Unfortunately, in the case of the HIV Tat protein, the contrast agent also was translocated to the nucleus, where interactions with DNA cannot be excluded. An ideal transfection agent will concentrate the contrast agent exclusively in the cytoplasm.

In order to achieve this, Gd can be attached to dendrimers, a macromolecule shaped like the branches of a tree that binds numerous Gd molecules [51]. These

molecules are internalized into the cytoplasm. A complementary method consists lipofection with Gd contrast agents. Lipofection is a method where contrast agent is encapsulated within cationic lipids. Cellular uptake involves non-specific interaction with the cell surface, endocytosis and release of contrast agent from the endosomal compartment [59]. This method has been used for both T_1 and T_2 contrast agents, and is also used to transfect DNA [30, 83].

Homing and engraftment of stem cells can be visualized using a variety of imaging methods, predominately through labeling cells prior to implantation. This constitutes a powerful tool for both researchers and clinicians, who now have non-invasive methods for studying what happens to stem cells once they are in the body.

Methods to Visualize Stem Cell Differentiation in vivo

With most therapeutic approaches involving stem cells, although we are interested where the stem cells migrate inside the body, of greater interest are questions regarding stem cells differentiation into target organ tissue. If we transplant neuronal stem cells into the brain following an ischemic insult, what kinds of cells arise? Neurons? Glial cells? Hepatocytes? To answer this question, it is necessary to know how differentiated cells differ from stem cells.

Differentiated cells usually possess tissue-specific morphology while stem cells do not. For example, neurons possess a distinct histological appearance consisting of dendrites, perikaryon and axons. If transplanted stem cells are labeled (for identification as implanted cells), injected into a tissue, explanted and viewed under a microscope, findings related to differentiation can be made. Neuroepithelial stem cells were harvested from a transgenic green fluorescent protein (GFP) rat and engrafted into a normal rat striatum [94]. Fluorescent microscopy of explanted tissue revealed implanted stem cell differentiation into neurons. Unfortunately, imaging cell histology in vivo is not possible. In addition, cell histology is not specific enough, for example there is little visible difference between an ES cell and a neural stem cell.

A better way is to take into account a cell's pattern of gene expression. Stem cells possess a different composition of expressed genes when compared to a differentiated cell. Proteins that are characteristically expressed by a specific cell population are called marker proteins. These marker proteins are fairly well characterized, and turn the problem of imaging cell differentiation into a problem of imaging gene expression. While constituting a gross simplification of the differentiation process, a summary of generally agreed upon markers of embryonic stem cells, neural stem cells and their progeny can be found in Figure 3.

Since most gene expression imaging research is associated with cancer research, most of the following examples will come from that field. Imaging a specific protein inside a cell is highly dependant on the properties of the protein. In isolated cases, the protein that is to be imaged displays inherent properties that allows it to be visualized directly. For MR imaging, this is the case with proteins having to do with iron metabolism, specifically ferritin and transferrin. Tumor cells that were genetically modified to express increased levels of transferrin were injected into mice [99]. Transferrin expression in cells caused a reduction of signal in T_2-weighted images.

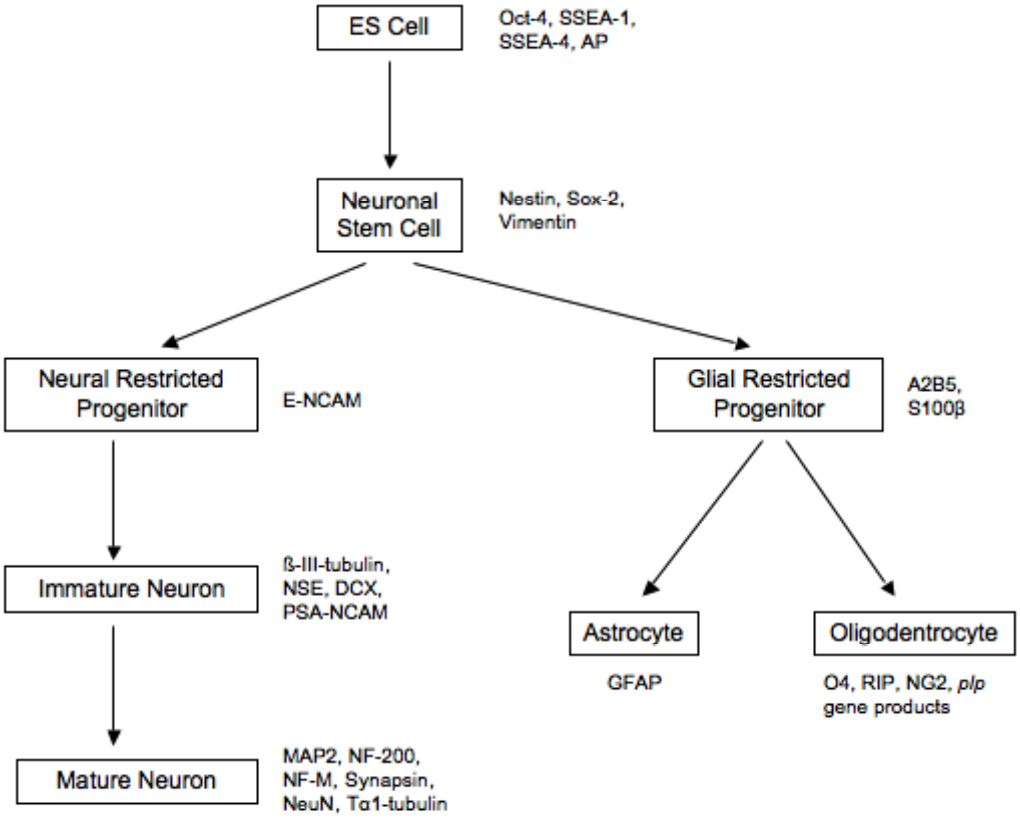

Figure 3 Common markers for stem cells, neuronal stem cells and their progeny. Adapted from **[9, 23, 25, 48, 56, 60, 73, 74, 79, 101]**.

Most of the time, unfortunately, we cannot count on markers having intrinsic imaging properties so we are required to use molecular biology tricks in order to visualize gene expression. Antibodies that bind specific antigens are routinely used to detect proteins. Ex vivo, antibodies bound with fluorescent dye are commonplace in histological diagnosis. In vivo, contrast agents can be bound to antibodies to visualize a specific protein. Quantum dots are novel fluorescent probes that are used in optical imaging [44]. They have been bound to antibodies to demonstrate detection of Her-2 [100], a marker for a type of breast cancer that correlates to poor prognosis, and prostate specific membrane antigen [33], a marker for prostate cancer. In MR imaging, monoclonal antibodies against Her-2/neu linked to a Gd chelate successfully imaged that protein expressed on the cell membrane [5].

Another method is to use the promoter of a marker and link it to a reporter gene. For example, if we wished to visualize an ES cell becoming a neuronal stem

cell, we could utilize the marker protein doublecortin. Since doublecortin is expressed in a neuronal stem cell but not in an ES cell*, the transcriptional factors that facilitate doublecortin expression must be active in a neuronal stem cell and inactive in an ES cell. If a reporter gene is placed under the promoter for doublecortin, it will only be transcribed when doublecortin is transcribed. Such a vector can be constructed using a layout depicted in Figure 4. We will be using a similar construct for our experiments.

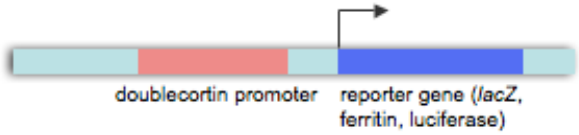

Figure 4 A possible vector construct to visualize the expression of doublecortin.

There has been much work done on labeling stem cells, unfortunately though, thorough studies have yet to be completed for the in vivo imaging of differentiation of stem cells. We have seen that imaging of gene expression is far from trivial and depends highly on the protein one wishes to visualize. It is hoped that this thesis paper will contribute to a solution for this problem.

Intelligent Contrast Agents

Methods to visualize stem cell differentiation in vivo demand intelligent contrast agents. There are generally three types of contrast agents, namely nonspecific, targeted and smart contrast agents [77]. Nonspecific contrast agents, such as Gd chelates (Figure 5), are widely in clinical use and enhance contrast in a nonspecific distribution pattern. Targeted contrast agents are linked to ligands of specific affinity. An example is the Her-2/neu specific antibody linked to a Gd

* Unfortunately, this is not black or white. While the majority of ES cells **do not** and the majority of neuronal stem cell **do** express doublecortin, there are small percentages of both cell populations that behave oppositely

chelate described previously [5]. Smart contrast agents display different signal-enhancing characteristics upon interaction with a specific target. This group of contrast agents is especially interesting for molecular imaging applications.

One approach in the field of optical imaging is demonstrated by the use of a reporter molecule that is cleaved by a specific caspase [55]. Caspases are a family of proteins involved in apoptosis, and as such are of interest for cancer researchers. Luciferase was bound to two estrogen receptor (ER) molecules by a specific peptide sequence that caspase-3 specifically splits. ER molecules successfully silenced the activity of the luciferase. When cells underwent apoptosis, caspase-3 was expressed. As a result, luciferase was set free by proteolysis of the bonds between the ERs and the reporting enzyme.

MR contrast agents require direct interaction with protons in water molecules to facilitate their effect. This interaction can be influenced in three different ways. One can vary the number of water molecules coordinated to the paramagnetic ion, the lifetime of the water molecule bound to the paramagnetic ion or the relaxivity of the complex [63]. These properties can be used to create agents that can be switched from an inactive into an active state. The Gd ion has 9 coordination sites. In its role as a nonspecific contrast agent, Gd is complexed by a chelator (DOTA or DTPA) in 8 coordination sites, leaving one coordination site to interact with water molecules (Figure 5). Most intelligent contrast agents are modified in this 9^{th} coordination site in order to become conditionally activated.

T_2 contrast agents have been developed that can visualize specific oligonucleotide sequences [46, 76]. Iron oxides cross-linked to a DNA sequence hybridized its complementary sequence in vitro and caused decreased signal intensity in T_2-weighted images. While constituting a targeted, not a smart contrast agent, this method may play a role in visualizing gene expression in the future. Thus far however, this technique has only been utilized for test solutions, not for intracellular DNA detection.

Intracellular calcium (Ca^{2+}) plays an important role in signal transduction. Li et al developed a contrast agent where a Ca^{2+} binding domain links two chelated Gd

ions [57]. When there is low Ca^{2+} in the cell, all coordination sites of the contrast agent molecule are bound to the Gd ions, as can be seen in (Figure 5). In this state, is it difficult for water to interact directly with Gd, therefore there is little contrast enhancement. When Ca^{2+} is introduced, it steals two coordination binds from the Gd ion and opens a pathway for water interaction. With high levels of Ca^{2+} the contrast agent is in its active state and there is an increased signal in MR.

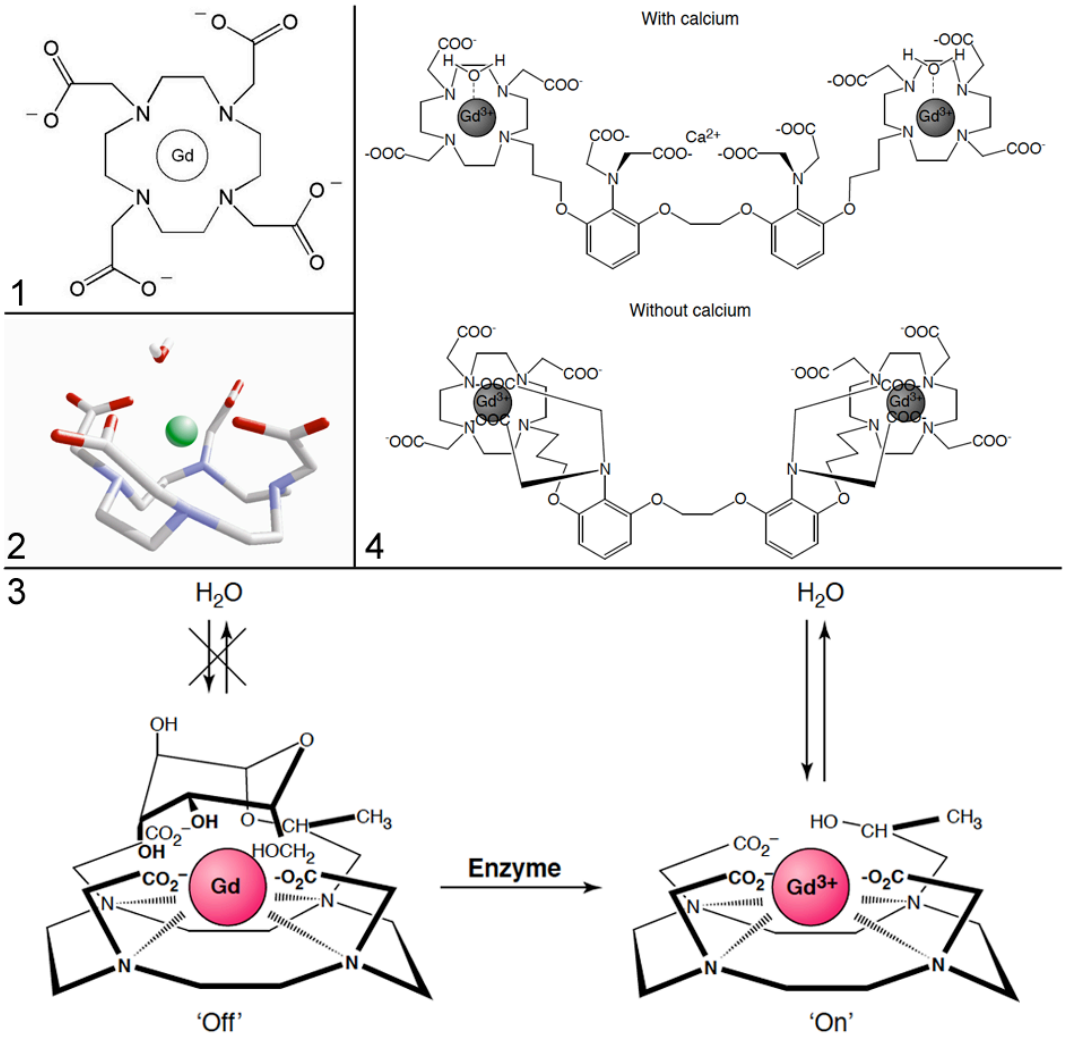

Figure 5 (1) Gd-DOTA, a common unspecific contrast agent (2) Rendering of Gd-DOTA showing the 3D structure of the complex. Note the free coordination site where the molecule interacts with water (3) Gd BAPTA-DO3A, a Ca^{2+} sensitive contrast agent. Note the "swivel arms" of the complex that can interact either with Ca^{2+} or Gd (4) The EgadMe molecule. In its inactive form, a galactopyranose ring blocks access of water. After cleavage with β-galactosidase, the complex is free to interact with water. (1), (2) from **[68]**, (3) from **[57]**, (4) from **[63]**.

For our experiments, we will be using a contrast agent known as EgadMe, which is based on the earlier generation EGad contrast agent first described by Moats et al in 1997 [66]. EgadMe consists of a molecule that chelates 8 of the 9 coordination sites of Gd and a galactopyranose ring that blocks the remaining coordination site. The galactopyranose ring can be cleaved by β-galactosidase, an enzyme that is encoded by the *lacZ* gene. Once the ring has been cleaved, water molecules can interact with Gd and increased signal intensity results in T_1-weighted images. Capillary tubes of EGad with and without β-galactosidase show very different contrast enhancement behavior (Figure 6).

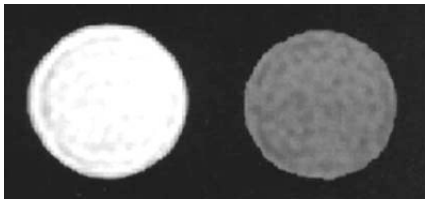

Figure 6 Capillary tubes with 2.0 μM EGad in presence (left) and absence (right) of 5.1 μM β-galactosidase. Note the significant difference in signal intensity in these T_1-wieghted IR sequences. From **[66]**.

EgadMe has been used in experiments to visualize gene expression in vivo [61]. Both cells of *Xenopus laevis* embryos in the two-cell phase were injected with EgadMe. One of the cells also received an injection with β-galactosidase mRNA. Since the first mitosis roughly splits the animal in two sides, the future embryo will have both EgadMe and β-galactosidase on one side and just EgadMe on the other. Since the cells that received mRNA express β-galactosidase as a result, those cells also contain cleaved, active EgadMe (Figure 7). Classical staining for β -galactosidase correlated well with MRI findings. In addition to injecting mRNA into the cell, the group also tested a plasmid that encoded *lacZ* with similar results.

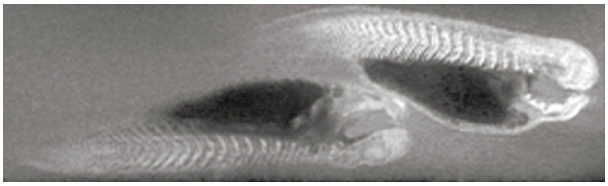

Figure 7 MR image of two *Xenopus laevis* embryos, left without β-galactosidase, right with β -galactosidase injected into one cell during the two-cell phase. Note the increase of signal intensity on only one side of the animal on the right. From **[61]**.

This shows that EgadMe combined with β-galactosidase is a powerful tool in visualizing gene expression in vivo. Combined with the methods introduced in the previous chapter, an approach for visualizing stem cell differentiation in vivo can be achieved. If we introduce a vector into a stem cell that has β-galactosidase under a marker gene promoter (such as doublecortin) and introduce EgadMe into the cell, upon stem cell differentiation, an increase in signal in T_1-weighted images is expected. It is the goal of this thesis paper to show just that.

Materials & Methods

Part 1 – Experiments with Adult Neural Stem Cells

The experiments within the scope of this thesis were completed using two different cell lines – mouse embryonic stem cells and mouse adult neuronal stem cells. Initial studies were performed with the goal of optimizing contrast agent labeling and MR scanning protocols. For these studies, a cell line that is readily obtained and easily cultured while displaying similar properties to the actual embryonic stem cells that are of interest was needed: the mouse adult neuronal stem cell. Subsequent studies were performed with the goal of visualizing the differentiation of stem cells labeled with contrast agent. These experiments were performed using mouse embryonic stem cells, and will be described later.

Adult neuronal stem cells in mammals can be found in two locations, the subventricular zone (SVZ) and the subgranular layer of the dentate gyrus [78]. In the brains of adult primates, SVZ cells constantly generate neuronal precursors that migrate to the olfactory bulb where they replace interneurons. SVZ cells are also known to generate glia cells. The fact that these cells display self-renewal and multipotency suggest that they are, in fact, true adult stem cells [2].

To obtain SVZ cells, young Balb-C mice were killed by cervical dislocation and were sterilized with ethanol. Craniotomy was performed, and the brain was sliced coronally in the region of the periventricular zone at a thickness of approximately 1 mm. Slices were immediately immersed in PIPES buffer (Sigma-Aldrich, St. Louis, Missouri, # 80636), a hydrogen-ion based organic buffer with a useful pH range between 6.4 and 7.2 [35]. Under a light microscope, a thin layer of tissue was scraped off the ventricular wall. The layers were then chopped down to a small size using a scalpel, suspended in Papain (Sigma-Aldrich, # P3250) and incubated for 25 minutes at 37°C. Papain is a cystein proteinase that breaks down the extracellular matrix molecules that hold cells together, facilitating the production of single cells required for cell culture [10]. Cells were then centrifuged (5 minutes at

200 rcf), resuspended in media, plated in 12-well plates and grown overnight at standard cell culture conditions (37°C, 5% CO_2, 95% relative humidity). The next day, non-adherent cells were collected and replated. Media was replaced every other day. Cells were split 1:4 using 0.05% Trypsin (Invitrogen, Carlsbad, California, # 25300-054) after having reached a confluency of 120%. The media used is as follows:

DMEM 50%/F12 50% (Invitrogen, # 11320-033)
Foetal Bovine Serum, Defined, 5% (HyClone, Logan, Utah, # SH30070.01)
N2 supplement, 10 µl/ml (Invitrogen, # 17502-048)
Bovine pituitary extract, 35µg/ml (Invitrogen, # 13028-014)
rhEGF, 20 ng/ml (Invitrogen, # 13247-051)
rhFGF basic, 20 ng/ml (Invitrogen, # 13256-029)
Amphotericin B, 250 mg/ml (Mediatech, Manassas, Virginia # 30-003-CF)
Penicillin/Streptomycin, 1% (Mediatech, # 30-002-CI)

Experiment 1 – Optimization of Cell Labeling with Gd-DTPA and Gd-DO3A

Rationale

Pilot studies were performed using conventional contrast agent labeling methods. The rationale behind these experiments was to determine if cells can be labeled and imaged using standard labeling methods. If the cells were labeled successfully, a rough estimate of the maximum possible signal effect of the EgadMe contrast agent can be deduced.

Cell Culture

SVZ cells were derived and cultured as previously described and were kindly provided by the Alvarez-Buylla Laboratory (UCSF).

Contrast Agent

Gd-DTPA (Gadophrin, Schering, Berlin, Germany) and Gd-DO3A (Gadoteridol, Bracco, Princeton, New Jersey) were used. Two contrast agents were used primarily to assess the differences in cellular uptake between negatively charged (Gd-DTPA) and neutrally charged (Gd-DO3A) molecules.

Gd-DTPA is a small weight (0.55 kDa) molecule that is used clinically as a non-specific contrast agent [85, 98]. The r_1 and r_2 relaxivities are 3.3 (3.1-3.5) and 3.9 (2.8-5.0) $mmol^{-1}s^{-1}$ in water at 37°C and 1.5 T respectively [81]. Gd-DTPA is a linear molecule and contains two negative charges. The structure of Gd-DTPA can be seen in Figure 8.

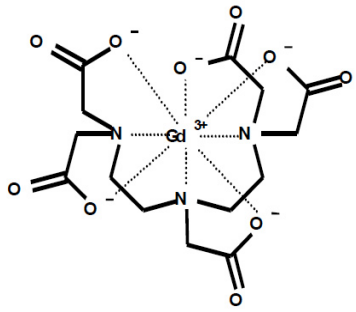

Figure 8 Structure of Gd-DTPA. Note the net double negative charge: 3 positive charges in the gadolinium ion, 5 negative charges in the DTPA ring. From **[12]**.

Gd-DO3A is a neutral, small molecular weight (0.56 kDa) contrast agent that is used clinically [64]. The r_1 and r_2 relaxivities are 2.9 (2.7-3.1) and 3.2 (2.5-3.9) $mmol^{-1}s^{-1}$ in water at 37°C and 1.5 T respectively [81]. The structure of the contrast agent molecule can be found in Figure 9. Gd-DO3A is structurally equivalent to EgadMe in its cleaved, activated form (Figure 5), making it optimal for preliminary testing of labeling efficiency.

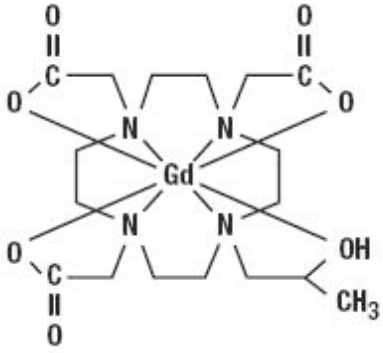

Figure 9 Structural formula of Gd-DO3A. Note the neutral charge (3 negative charges from DO3A and 3 positive charges from Gd) and the similarities to EgadMe in its cleaved form. From **[64]**.

Transfection Agent

In order to facilitate efficient transfection of the contrast agent into SVZ cells, Lipofectin (Invitrogen, # 18292-011) was used. Lipofectin is a reagent consisting of the cationic lipids DOTMA and DOPE in a 1:1 mixture in membrane-filtered water [83]. The structural formula can be seen in Figure 10. The classical use of lipofectin is to transfect DNA or RNA, however lipid-mediated transfection has also been used in cell labeling with contrast agents [20]. While most studies concerning the mechanism of cellular uptake with lipofectin use DNA and not MR contrast agents, it is likely that multiple positively charged lipid molecules form complexes with the negatively charged contrast agent [27]. The complexes then fuse with the cell membrane and deliver the contents into the cytosol.

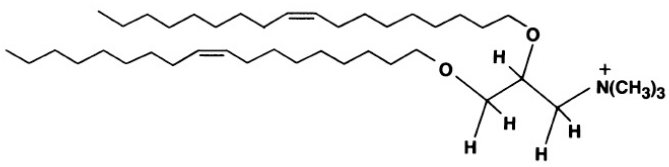

Figure 10 Structure of DOTMA. Note the positive charge that allows complex formation with negatively charged molecules and the lipophilic tail that enables liposome formation.

Labeling Protocol

Labeling of SVZ cells with Gd-DTPA and Gd-DO3A was done as follows: SVZ cells were plated to 80% confluency and allowed to adhere overnight. Two solutions were prepared, one with lipofectin (20 µl of reagent in 100 µl DMEM) and one with either 37.5 µmol Gd-DTPA or Gd-DO3A (75 µl of 0.5 M contrast agent in 100 µl DMEM). After 30 minutes, both solutions were mixed gently to allow complex formation and allowed to incubate at room temperature for 45 minutes. The solution was then introduced into the culture flask that contained the previously described culture media and was incubated at standard cell culture conditions for 5 hours. After incubation, supernatant was removed and cells were rinsed with PBS. Cells were trypsinized and washed by centrifugation (400 xg, 5 min, 25°C) 3 times to ensure that all remaining extracellular contrast agent was removed. Cells were then prepared for MR scanning by resuspending 10^6 cells in 75 µl agarose (Sigma-Aldrich, # A2576) in 500 µl Eppendorf tubes (VWR, West Chester, Pennsylvania, # 89000).

Cell Viability Measurement

To ensure that the contrast agent labeling process itself is not toxic to the cell, trypan blue exclusion staining was performed before and after labeling. Trypan blue is a vital dye. The reactivity is based on the fact that the dye is negatively charged and does not interact with the cell unless the membrane is damaged [32]. Cells that exclude the dye are viable whereas cells that stain blue are not. To perform viability testing, 20 µl of cell suspension and 20 µl Trypan blue staining solution (Invitrogen, # 15250-061) were combined and incubated at room temperature for 5 minutes. A Neubauer cell counting chamber was filled with the combined solution and examined under a light microscope. The ratio of non-viable to viable cells was calculated.

MR Imaging Protocol

MR imaging of the Eppendorf tubes was performed using clinical MR Scanners operating at 1.5 T (Signa EXCITE HD 1.5 T, GE Medical Systems, Milwaukee, Wisconsin) and standard circularly polarized quadrature knee coils (Clinical MR Solutions, Brookfield, Wisconsin). To avoid susceptibility artifacts from the surrounding air while scanning, all probes were placed in a water-containing

plastic container. To minimize image distortion due to vibration induced by the MR scanning procedure, generous padding below and above the container was introduced. An image of the experimental setup can be found in Figure 11. All probes were evaluated at room temperature (20ºC).

Samples of cells suspended in agarose were investigated with spin-echo (SE) and gradient echo (GE) sequences. In order to quantify T_1 relaxation times, SE images with TR values of 4000, 1000, 500, 250 ms and a TE of 15 ms were obtained. For calculation of T_2 relaxation times, SE images with TE values of 60, 45, 30, 15 ms and a TR of 4000 ms were acquired using 4 echos. T_2^* quantification was done using GE images with TE values of 28.8, 14.4, 7.2, 3.7 ms, a TR of 500 ms and a flip angle of 30°. All sequences were acquired with a field of view (FOV) of 12 x12 cm, a matrix of 256x196 pixel, a slice thickness of 5 mm and one acquisition.

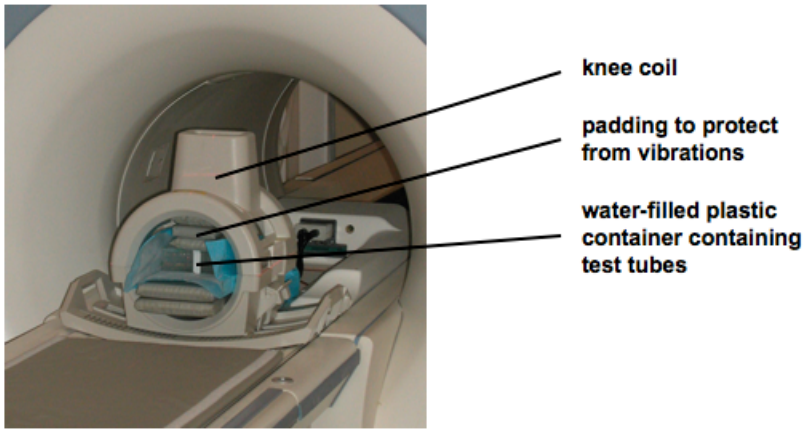

Figure 11 Picture of the experimental setup while scanning.

MR Data Analysis

Images were analyzed qualitatively by determining any visible contrast agent effect in labeled versus non-labeled cell suspensions. For this analysis, T_1-weighted images were derived from the SE sequence (TE 15 ms, TR 500 ms), T_2-weighted images were derived from the SE sequence (TE 60 ms, TR 4000 ms, 4 echos) and T_2^*-weighted images were derived from the GE sequence (TE 3.2 ms, TR 500 ms, flip angle 30°).

For quantitative data analysis, MR images were transferred as DICOM images to a SUN/SPARC workstation (Sun Microsystems, Mountain View, California) and processed by a self-written IDL program (Interactive Data Language, Research Systems, Boulder, Colorado). The IDL program determines the T_1, T_2 or T_2^* relaxation times of each pixel by fitting the signal intensities from 4 images with varying MR scan parameters onto a monoexponential signal decay curve using nonlinear function least-square curve fitting on a pixel-by-pixel basis. The program outputs a map image that depicts the relaxation times for each pixel. Regions of interest (ROI) are then placed into the map image and relaxation time of each ROI is calculated by averaging the relaxation times of individual pixels in the ROI. Care was taken to analyze only data points with signal intensities significantly above the noise level. A schematic of this process is depicted in Figure 12.

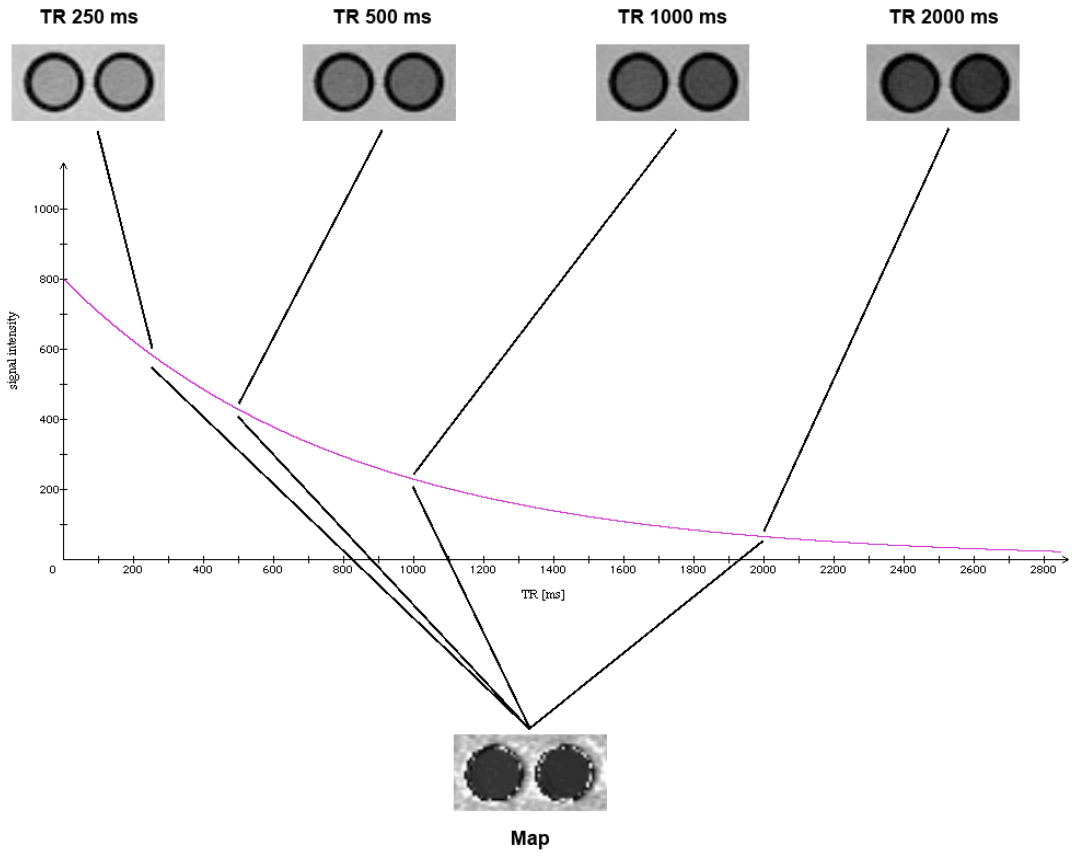

Figure 12 Schematic of the calculation of relaxation times are. In this image, T_2 relaxation times for each pixel are fitted to the T_2 signal decay curve. The result is a T_2 map, which is a depiction of the T_2 time of each pixel. The T_2 times of each pixel in a region of interest that corresponds to an Eppendorf tube are then averaged and outputted.

T_1 maps were calculated from four SE images with a fixed TE of 15 ms and variable TR values of 4000, 1000, 500 and 250 ms, T_2 maps from SE images with a fixed TR of 4000 ms, variable TE values of 60, 45, 30 and 15 ms an 4 echos and T_2^* maps from GE images with a fixed TR of 500 ms, variable TE values of 28.8, 14.4, 7.2 and 3.7 ms and a flip angle of 30°. The signal intensity (SI) for each pixel as a function of time (t) was expressed as follows for T_1: $SI_z(t) = S_0(1 - e^{-\frac{t}{T_1}})$. For T_2 and T_2^* the function was as follows: $SI_{xy}(t) = S_0 \cdot e^{-\frac{t}{T_2}}$

Endpoints

The endpoint of this experiment was to establish a protocol for labeling and imaging SVZ cells with gadolinium-based contrast agents. The results will aid in performing further experiments using the "smart" EgadMe contrast agent.

Experiment 2 – Creating a β-galactosidase Expressing Adult Neural Stem Cell Line

Rationale

The previous experiment showed that SVZ cells are successfully labeled with a gadolinium-based contrast agent similar in structure to EgadMe. The goal of the next experiment was to create a population of adult neural stem cells that express β-galactosidase. This cell population will be tested against a β-galactosidase-negative adult neural stem cell line concerning contrast enhancement with EgadMe labeling.

Vector Construct and Transfection

SVZ cells were transfected to the effect where one population expressed *lacZ* and the other did not. SVZ cells were harvested from a ROSA26-Cre reporter mouse strain kindly provided by the Alvarez-Buylla Laboratory (UCSF). The ROSA26-Cre reporter strain was created by gene trapping the ROSA26 locus, a locus which is

expressed ubiquitously in all cells during embryonic development [89]. Gene trapping is a method where a reporter gene, such as lacZ, is randomly integrated into the genome [102]. When the targeted gene is expressed, lacZ is expressed concurrently, shedding insight as to when gene expression occurs during embryogenesis. Cre is a DNA recombinase that catalyzes DNA recombination between two 34-base pair nucleotide sequences known as loxP sites [53]. In the ROSA26-Cre reporter strain, a neo resistance cassette was floxed (that is flanked by two loxP sites) and flanked by the reporter gene *lacZ*, and as such did not have active β-galactosidase production. A neo resistance cassette confers resistance to neomycin and is used for selection of properly transfected cells. Cells with a correct transfection express the neo resistance and do not die upon neomycin treatment whereas incorrectly transfected cells perish. Upon transfection with an adenoviral Cre vector, Ad5-CMV-Cre (CAGT Vector Development Laboratory, Baylor College of Medicine, Houston, Texas), Cre is expressed inside the cell. The Cre recombinase deletes the floxed neo resistance cassette and allows the reporter gene *lacZ* to become expressed. A simplified schematic is found in Figure 13.

Transfection with the Ad5-CMV-Cre vector was done as follows: Adenoviral vector was provided at a concentration of 5.0×10^{12} particles/ml in a storage buffer of 20 mM HEPES buffer at a pH of 7.8 in 150 mM NaCl with 10% glycerol and was stored at -80°C. Cells were coated with growth factor free and serum free medium at approximately 100 µl medium per 1 cm^2 flask area. 5 µl virus stock solution (approximately 2500 virus particles per cell) and 100 µl medium per 1 cm^2 flask area of full medium was added and subsequently incubated for 6 hours at standard cell culture condition after which the medium was changed.

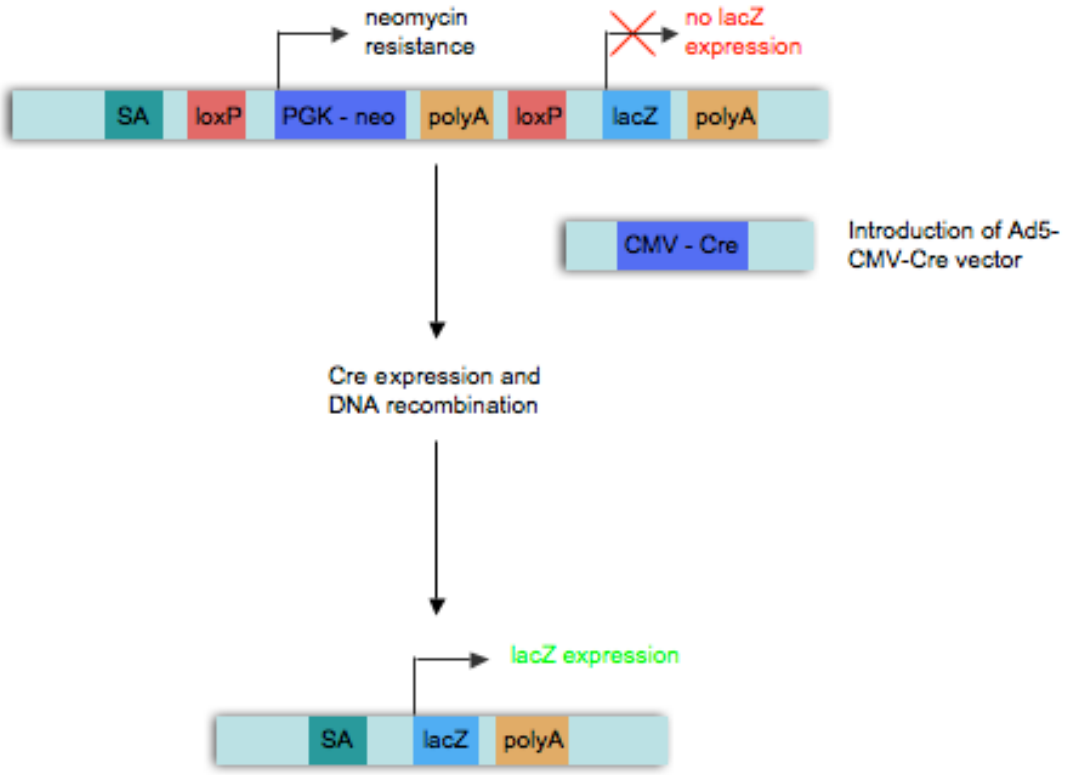

Figure 13 Scematic of the mechanism of lacZ expression in the ROSA26-Cre strain. Prior to introduction of the Ad5-CMV-Cre vector, only the neomycin resistance gene is expressed. The Ad5 vector enters the cell and expresses Cre which excises the floxed genetic material, that is, the PGK-neo and polyA which is in between two loxP sites. After recombination, the cells express lacZ.

Xgal Staining

To prove successful transfection, the Xgal stain was used. The Xgal stain is a common histological method of showing that cells produce β-galactosidase. In this staining method, cells are treated with a substrate which has galactose linked through a β-D-glycosidic linkage [13]. The properties of this substance change upon the liberation from galactose by the β-galactosidase. The most common substance used is Xgal [40]. With Xgal, upon cleavage, a soluble, colorless monomer is produced. When two of these monomers react, a blue halogenated indigo result that is stable. In

order for the dimerization and oxidation to work, ferric and ferrous ions such as potassium ferricyanide and potassium ferrocyanide are usually added to the reagent mixture. A schematic of the staining reaction is found in Figure 14.

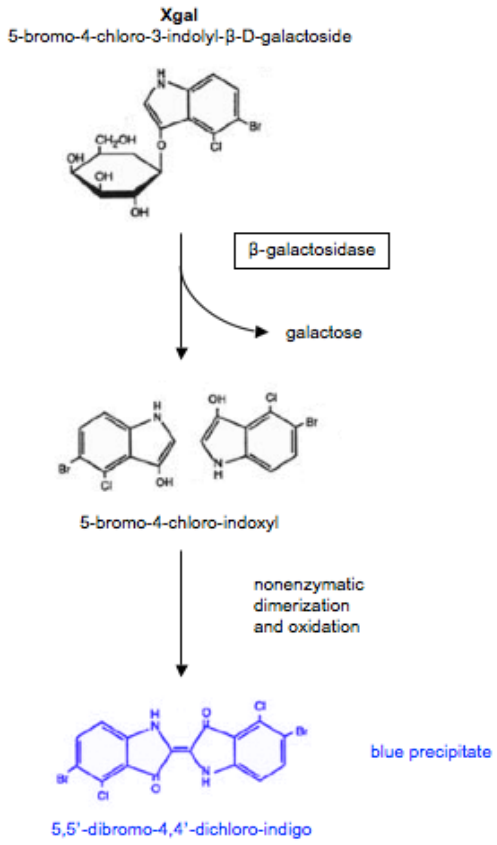

Figure 14 Schematic of the Xgal staining reaction. Adapted from **[13]**.

Xgal staining was performed using the Xgal staining assay kit (Gene Therapy Systems, San Diego, California, # A10300K) that contained fixing buffer, staining buffer and Xgal stock solution. Medium was aspirated and adherent cells were washed once with PBS solution. Fixing buffer was added to the dish at 100 µl per cm^2 area and incubated for 15 minutes at room temperature. Fixing buffer was removed and cells were washed twice with PBS. Xgal staining solution was prepared by diluting Xgal stock solution 1:25 with staining buffer. Fresh Xgal staining solution was introduced to the dish at 100 µl per cm^2 and incubated at standard cell culture conditions for 1 to 18 hours, depending on the transfection efficiency of β-galactosidase. Xgal staining solution was removed and washed once with PBS. Stained cells were then examined under a light microscope.

Endpoints

The endpoint of this experiment was to create an adult neural stem cell line that expresses β-galactosidase that will be labeled with EgadMe, subsequently imaged and compared with an identical cell line that does not express the enzyme.

Experiment 3 – EgadMe Labeling and MR Imaging with β-galactosidase Positive and Negative Adult Neural Stem Cells

Rationale

Labeling β-galactosidase positive and negative cells with EgadMe will permit conclusions concerning the signal enhancement effects of the inactive, uncleaved form compared to the active, cleaved form of this "smart" contrast agent. This will aid in adapting MR imaging sequences to properly detect the changes in signal intensity.

EgadMe Contrast Agent

EgadMe (1-[2-(-galactopyranosyloxy)propyl]-4,7,10-tris(carboxymethyl)-1,4,7,10-tetraazacyclododecane) gadolinium(III) complex) is a contrast agent sensitive to β-galactosidase cleavage [1]. It has a molecular weight of 721 Da. The chemical structure can be seen in Figure 5. The ratio of T_1 times of the active and inactive forms of EgadMe was measured to be 49% where $T_{1\ cleaved}$ = 0.56 s and $T_{1\ uncleaved}$ = 1.14 s (0.5 mM EgadMe in water in presence or absence of 4.3 μM β-galactosidase) [61]. Transfection was performed using the lipid-based transfection agent lipofectin as described previously.

Labeling Protocol

SVZ cells were plated at 80% confluency let to adhere overnight. The next day, labeling solutions were created with lipofectin (20 μl) and EgadMe (1.79

μmol/ml Gd) as described previously. Labeling solution was introduced to serum-free and antibiotic-free medium and incubated for 4 hours at standard cell culture conditions. Cells were then washed three times in PBS as previously described. In order to properly quantify effects on relaxation times, 9.85 x 10^6 cells were prepared as cell pellets or resuspended in 150 or 400 μl of ficoll (Sigma-Aldrich # F2637) prior to imaging. Ficoll is a neutral, highly branched, high mass hydrophilic polysaccharide that allows for homogenous dispersion of cells and preserves cell viability during scanning [38]. Ficoll was prepared with a density of 1.07 g/ml, a value that has proven useful for cell scanning purposes.

MR scanning parameters were completed as previously described.

Endpoints

The endpoints of this experiment was to show that SVZ cells internalize EgadMe, display an effect on relaxation time and vary in effect depending on SVZ expression of *lacZ*.

Experiment 4 – EgadMe Labeling at Various Concentrations and Long-Term Follow-Up

Rationale

Labeling β-galactosidase positive and negative SVZ cells with varying concentrations of EgadMe will allow conclusions as to the optimal EgadMe labeling concentration. Long-term follow-up will provide insight as to how long contrast agent effect is expected to persist once internalized.

Labeling Protocol

SVZ labeling was performed as previously described. Labeling solutions were composed of lipofectin (6.4 μl solution per μmol Gd) and increasing concentrations of EgadMe (0.22, 0.44, 0.89, 1.79 μmol/ml Gd). After 4 hours of incubation, cells were

washed three times in PBS and placed back into cell culture for 12 hours in order to allow ample time for the β-galactosidase to cleave internalized EgadMe. Cell viability was performed via Trypan Blue exclusion testing. 1.2 x 10^7 cells were then prepared for MR scanning by centrifugation into a cell pellet. After scanning, cells were resuspended in medium and cultured for an additional 9 days, after which 1.2 x 10^7 cells were prepared for MR scanning.

Spectrometry

In order to quantify the amount of contrast agent internalized by the cell, inductively coupled plasma atomic emission spectrometry (ICP-AES) was performed of cell samples after Day 9. ICP-AES is a technique that exploits the fact that excited electrons emit energy at a characteristic wavelength for each element as they return to their ground state [69]. The intensity of the energy emitted is proportional to the concentration of the element in the analyzed sample. Cells in the test sample were dissolved in a microwave (400 W, 55 min) after addition of 65% HNO_3 and 30% H_2O_2. The now dissolved samples were nebulized into an argon plasma and analyzed in a spectrometer (IRIS Advantage, Thermo Jarrell Ash, Waltham, Massachusetts). ICP-AES analysis was performed by collaborators from Schering AG who were blinded with respect to the contents of the samples.

Cell viability testing and MR scanning parameters were completed as previously described.

Endpoints

The endpoints of this experiment was to determine, based on preliminary experiments with similar contrast agents (Gd-DO3A), the optimal labeling parameters (EgadMe concentration and incubation time) for labeling of SVZ cells. In addition, the difference in signal intensity between β-galactosidase positive and negative cells was determined. Finally, long-term labeling efficiency was tested.

Part 2 – Experiments with Embryonic Stem Cells

Mouse embryonic stem (ES) cells were used for imaging studies of differentiated and non-differentiated neuronal cells. ES cells were introduced with a vector that conditionally expresses the reporter gene *lacZ* when the doublecortin (Dcx) promoter is active. Mouse ES cells were kindly provided by the Wynshaw-Boris Laboratory. Obtaining ES cells from the inner cell mass of a preimplantation blastocyst was first described by Evans et al in 1981 [26]. Briefly, mice from the 129 strain were mated. Three days later, implantation of the blastocyst was delayed by ovariectomy and injection with a progesterone-containing contraceptive agent [70]. Four days later, blastocysts were flushed from the uterus and transferred to a gelatin-coated plate (Sigma-Aldrich, # G1393). After five days of culture, the inner cell mass was disaggregated by physical dislodgement from the trophoblast with a fine glass rod and transferred into trypsin. Cells were dissociated into small groups, plated onto gelatinized culture wells and allowed to culture. Approximately one week later, once individual stem cell colonies contained 50-250 cells, they were dissociated using trypsin and repeated aspiration and replated onto gelatin-coated wells. A schematic can be seen in Figure 15. Of note, ES cells used were not feeder-layer dependant but instead used leukemia inhibitory factor (LIF) to prevent differentiation. Feeder cells are a layer of inactivated embryonic fibroblasts that coat the entire culture plate. ES cells attach on top of these feeder cells and experience inhibition of differentiation by substances that the feeder cells emit. Cells were split every two days, the medium changed on alternate days. The medium used is as follows:

DMEM, Optimized for ES cells (ATCC, # SCRR-2010)
FBS, ESC qualified, 15% (ATCC, # SCRR-30-2020, Lot # 300300)
L-Glutamine, 0.2 M, 2% (Invotrogen, # 25030-081)
NEAA (non-essential amino acids), 1% (Mediatech, # 25-025-CI)
Penicillin/Streptomycin, 1% (Mediatech, # 30-002-CI)
2-Mercaptoethanol, 10 mM, 1% (Invitrogen, # 31350-010)
ESGRO LIF, 1000 units/ml (Chemicon, Billerica, Massachusetts, # ESG1106)

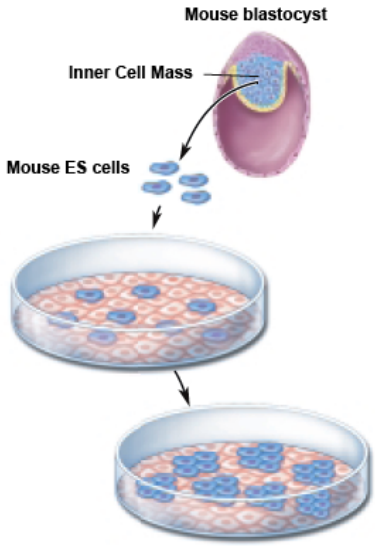

Figure 15 Schematic of the creation of a mouse ES primary culture. Note that in this picture a feeder cell layer was used whereas the ES cells used in this thesis are non-feeder dependant. From **[37]**.

Experiment 5 – Differentiation of ES Cells into Neurons

Rationale

Before EgadMe labeling of ES cells, it was necessary to demonstrate conditional expression of β-galactosidase upon neuronal differentiation using standard methods.

Vector Construct and Transfection

ES cells were transfected with a vector to the effect where β-galactosidase is expressed when the Dcx promoter is active, which occurs upon neural differentiation [15]. Transfection was performed by the Wynshaw-Boris Laboratory. The vector construct used is shown in Figure 16. When the Dcx promoter is active, recombinant cells express *lacZ* instead of expressing Dcx. Transfection was done via electroporation, a method where an electric pulse perturbs the cell membrane which forms a pore that allows nucleic acid to pass into the cell [97]. Addition of neomycin into the medium allows for selection of cells with successful transfection.

Approximately 8 days after electroporation successfully transfected ES colonies appear which are subsequently expanded to provide sufficient amounts of cells.

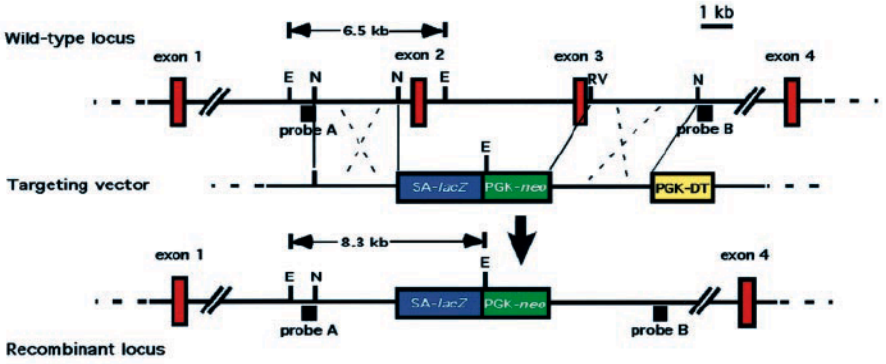

Figure 16 Schematic of the ES cell transfection. The targeting vector contains a splice acceptor (SA) and *lacZ* in addition to a neomycin resistance gene driven by a PGK enhancer. A splice acceptor is necessary as the genetic material integrates into an intron. Without a splice acceptor, *lacZ* would be transcribed into mRNA but not translated into protein as introns are removed from mRNA. The PGK enhancer is ubiquitously active and facilitates efficient transcription of the neomycin resistance gene. The targeting vector is integrated into an intron of the Dcx gene via homologous recombination. From **[15, 22]**.

Differentiation Protocol

Differentiation of ES cells into a neuronal lineage was performed via formation of embryoid bodies (EB). Embryoid bodies are cell aggregates that arise when ES cells are cultured without a feeder layer or LIF and contain tissue of the endoderm, mesoderm and ectoderm [37]. EB formation is facilitated when ES colonies are cultured in conditions where colonies are free-floating, classically as hanging drops. Alternatively, as was done in this thesis, EBs can be formed by plating ES cells onto dishes that do not allow ES cells to adhere to the dish surface. 3 x 10^6 ES cells were transferred into a 10 cm low attachment dish (Ultra Low Attachment Culture Dish, Corning, Corning, New York, # 3262) and cultures for two days with ES medium without LIF. Medium change was performed every other day by transferring EBs into a 15 ml tube, allowing EBs to settle by gravitation, aspiration of medium and replating into a low attachment dish with fresh, LIF-free ES medium. On day four the ES medium was supplemented with 5 µM of retinoic acid (Sigma-

Aldrich, # R2625). On day eight, cells were dispersed into single cells by resuspending EBs in trypsin and subsequent incubation for 10 minutes at 37°C. Cells were filtered through a 40 μm nylon mesh (BD Falcon, San Jose, California, # 352340) and collected by centrifugation. Cells were then resuspended in NBA/N2 medium and plated at a density of 10^6 cells per 10 cm^2 dish.

Detecting Neuronal Differentiation

At the end of the differentiation process, cells were analyzed for neuronal differentiation morphologically. Additionally, Xgal staining was performed to visualize β-galactosidase activity.

Endpoints

The primary endpoint of this experiment was to demonstrate ES cells in an undifferentiated, non *lacZ* expressing state and ES cells after differentiation into neuronal precursors with *lacZ* expression. The cells produced from this experiment will allow for labeling with EgadMe.

Experiment 6 – Detecting ES Cell Differentiation via MR Scanning with EgadMe

Rationale

The following experiment constitutes the primary endpoint of this thesis paper. ES cells were labeled at different point in the differentiation process – as β-galactosidase negative undifferentiated ES cells and as β-galactosidase positive differentiated ES cells.

Labeling protocol

Labeling protocols for ES cells were adapted from the previously described labeling protocols for PVZ cells. 1.5 x 10^7 β-galactosidase negative and positive ES

cells were labeled (0.22 μmol/ml EgadMe, 14.74 μg lipofectin solution, 12 hours incubation time) and centrifuged to cell pellets for MR scanning.

MR scanning parameters and were completed as previously described.

Endpoints

The endpoint of this experiment was to detect a difference in signal intensities of EgadMe labeled differentiated and undifferentiated stem cells.

Results

Part 1 – Experiments with Adult Neural Stem Cells

Experiment 1 – Optimization of Cell Labeling with Gd-DTPA and Gd-DO3A

The preliminary experiment utilized SVZ cells and established cell labeling methods in order to provide a rough estimate of labeling efficiency and expected signal behavior in the MR scanner. In addition, the comparison of Gd-DTPA and Gd-DO3A gives a slight insight on whether EgadMe – closely related in structure to Gd-DO3A – is efficiently internalized by cells. Three samples were tested: unlabeled control cells, cells labeled with Gd-DTPA and cells labeled with Gd-DO3A.

Cell Viability Measurement

Cell viability as measured via Trypan blue exclusion showed similar results between all three samples and were greater than 90%.

MR Imaging

On qualitative T_1-weighted images, both labeled cells showed increased signal intensity compared with unlabeled controls (Figure 17). Of the labeled cells, Gd-DO3A showed a higher effect on signal intensity than Gd-DTPA.

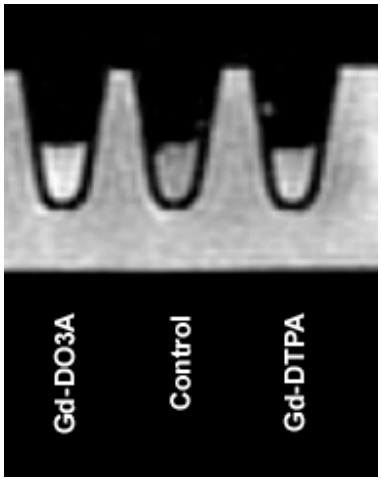

Figure 17 T_1-weighted SE (TE 15, TR 750) image of 10^6 SVZ cells labeled with either Gd-DTPA and lipofectin or Gd-DO3A and lipofectin in 75 µl agarose.

MR Data Analysis

As expected from the qualitative images, the samples labeled with contrast agent exhibited lower T_1 relaxation times when compared to the non-labeled control (Table 1). The contrast agent effect displayed by Gd-DO3A was greater than seen with Gd-DTPA.

	Gd-DO3A	Control	Gd-DTPA
T_1 [ms]	1480	3669	2387

Table 1 T_1 relaxation times of SVZ cell samples labeled with different contrast agents at 1.5 T.

Experiment 2 – Creating a β-galactosidase Expressing Adult Neural Stem Cell Line

SVZ cells were transfected with the Ad5 vector as described above. To prove successful transfection, Xgal staining was performed (Figure 18). SVZ cells that were not transfected showed no staining while transfected cells showed an intense

staining pattern. This shows that the majority of transfected cells express β-galactosidase after transfection.

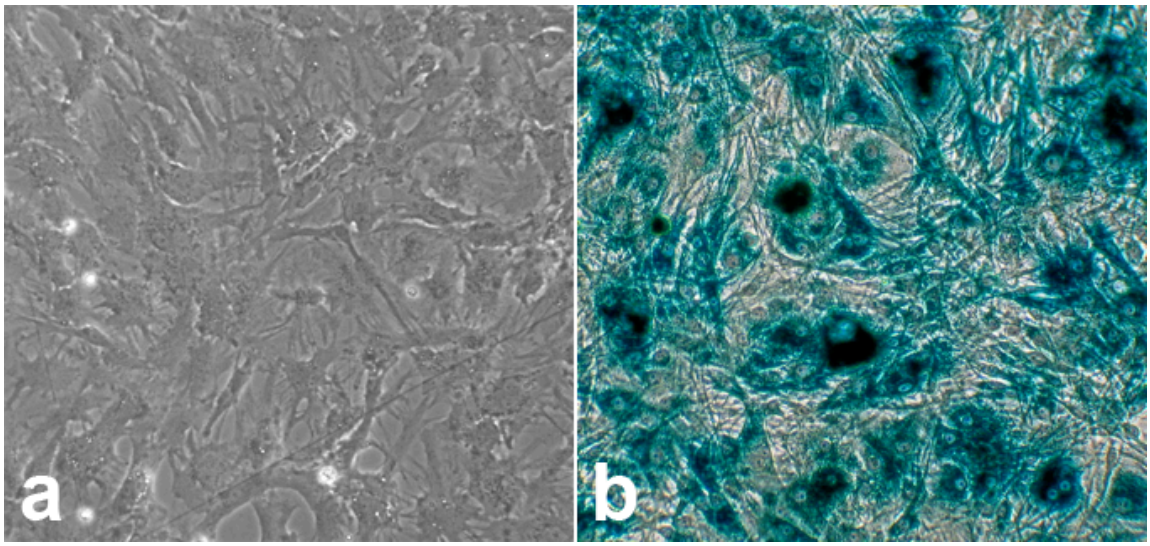

Figure 18 Light microscopy of transfected SVZ cells before (a) and after Xgal staining (b).

Experiment 3 – EgadMe Labeling and MR Imaging with β-galactosidase Positive and Negative Adult Neural Stem Cells

lacZ positive and negative SVZ cells were labeled with EgadMe and imaged in order to provide clues as to the signal characteristics of intracellular cleaved versus uncleaved EgadMe.

MR Imaging

Imaging was done of cell pellets and cells resuspended in 150 and 400 μl ficoll (Figure 19). While one can clearly see increased signal intensity in the β-galactosidase positive cell pellet, the differences where labeled cells are suspended in ficoll are more subtle.

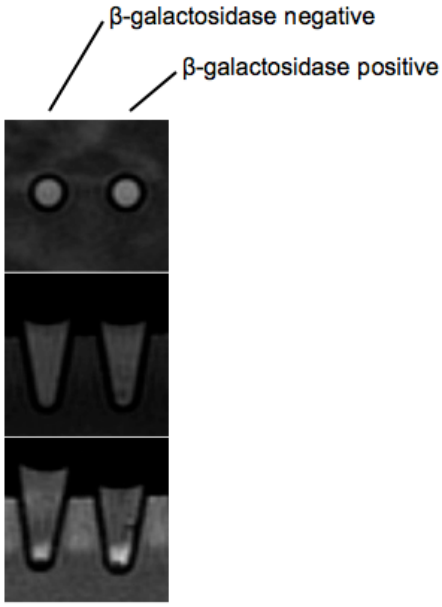

Figure 19 9.85 x 10^6 *lacZ* positive and negative SVZ cells labeled with EgadMe in T_1-weighted MR imaging (SE, TE 15, TR 500). Cells are suspended in 150 and 400 µl ficoll in the top and middle images, respectively, and are in pellets on the bottom image.

Experiment 4 – EgadMe Labeling at Various Concentrations and Long-Term Follow-Up

SVZ cells that expressed β-galactosidase were labeled with varying concentrations of EgadMe and compared with cells that did not express β-galactosidase in order to find an optimal labeling concentration. Labeling, scanning and viability measurement was performed at Day 0 and at Day 9. Spectrometry was performed in order to quantify the amount of contrast agent internalized by the cells.

MR Imaging

On qualitative T_1-weighted SE images (Figure 22), at Day 0, increasing concentration of EgadMe resulted in increased signal on T_1-weighted imaging with a maximum increase of signal seen with the highest concentration (1.79 µmol/ml). Compared to the unlabeled control, labeled cell pellets appear brighter and fuller. At Day 9, there is no noticeable difference seen between labeled and unlabeled cells.

Samples from Day 9 are less intense than samples from Day 0, including the unlabeled controls.

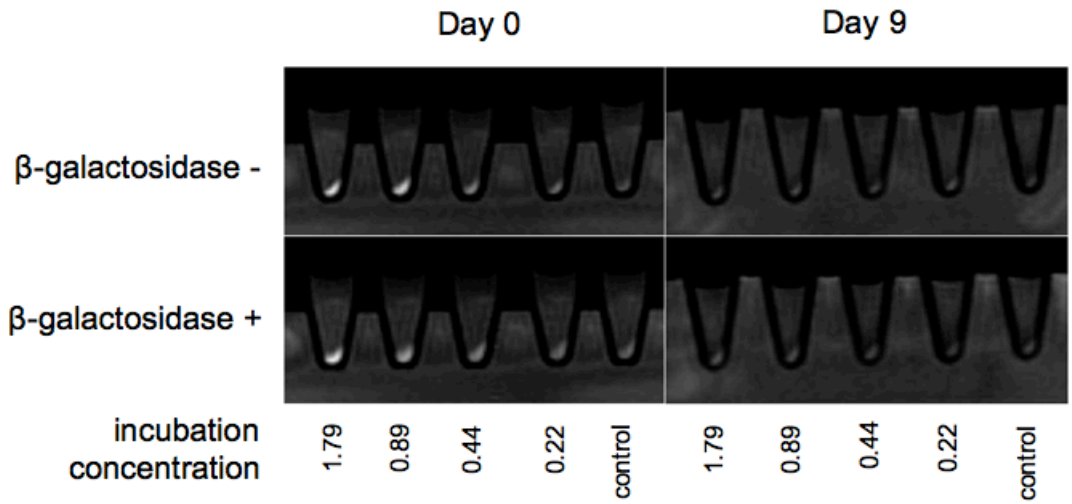

Figure 20 T_1-weighted SE images (TE 15, TR 500) of $1.2x10^7$ β-galactosidase positive and negative SVZ cells labeled with EgadMe at various concentrations at Day 0 and Day 9. Incubation concentration is [μmol/ml].

Cell Viability

After labeling, Trypan Blue exclusion testing was performed in order to assess cell viability (Figure 21). The β-galactosidase positive SVZ cells display poorer viability when compared to the β-galactosidase negative cells.

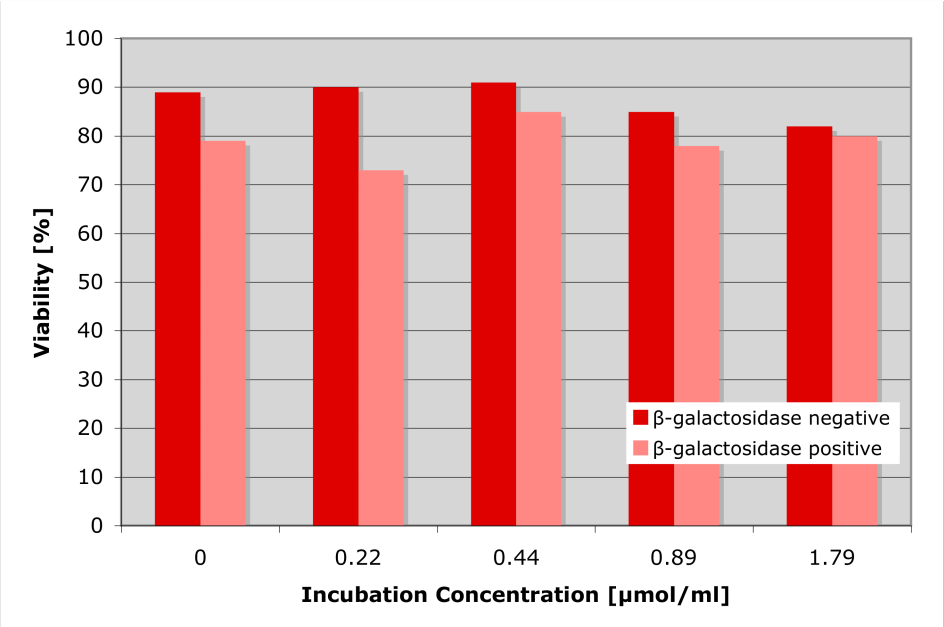

Figure 21 Cell viability after labeling at increasing concentrations of EgadMe.

MR Data Analysis

The quantitative measurement of the T_1 times corroborates the qualitative findings (Figure 22). The greatest difference between labeled β-galactosidase positive and negative SVZ cells at Day 0 is seen with the lowest concentration (0.22 µmol/ml). The difference between labeled β-galactosidase positive and negative SVZ cells becomes less obvious with higher labeling concentrations. Curiously there is a significant difference between unlabeled β-galactosidase positive and negative SVZ cells at Day 9.

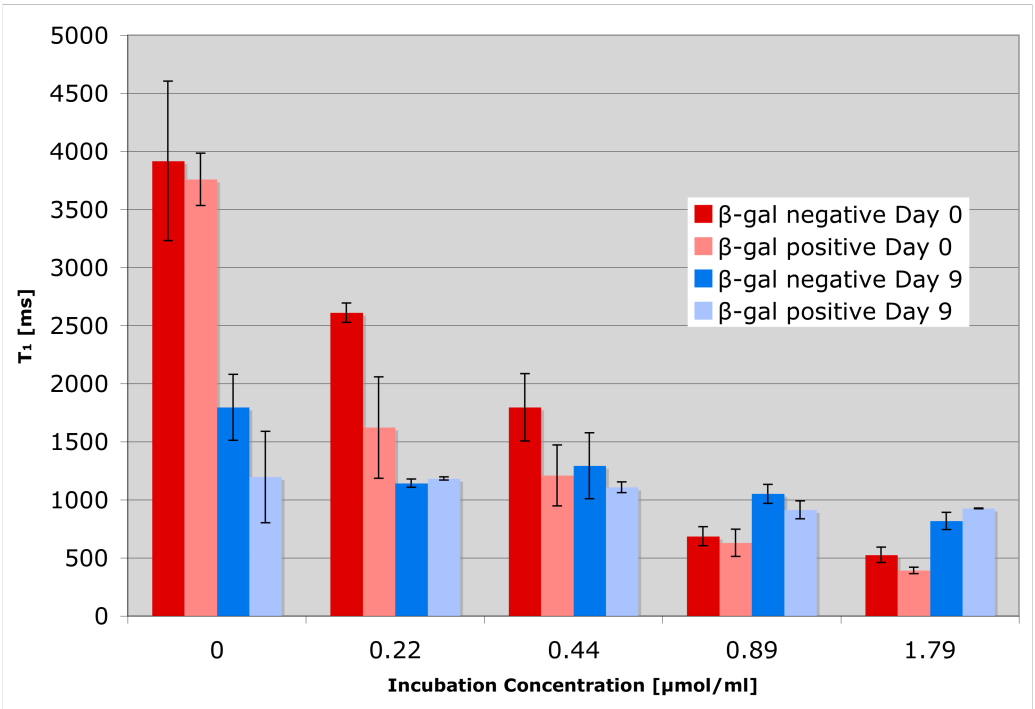

Figure 22 Measured T_1 relaxation times for β-galactosidase positive and negative SVZ cells at Day 0 and Day 9.

Spectrometry

The results of the ICP-AES analysis of the labeled cells after labeling, 9 days of culture and scanning is shown in (Table 2). Cells labeled at higher concentrations of EgadMe displayed higher concentrations of Gd on ICP-AES. β-galactosidase negative and positive cells share similar contrast agent uptake values when incubated at lower concentrations (0.22 and 0.44 µmol/ml) while β-galactosidase positive cells display poorer uptake at higher concentrations (0.89 and 1.79 µmol/ml). Interestingly there was a small amount of Gd measured in the unlabeled β-galactosidase positive control.

Incubation Concentration [µmol/ml]	β-galactosidase negative SVZ		β-galactosidase positive SVZ	
	Gd Amount in Sample [nmol]	Gd Amount per Cell [fmol/cell]	Gd Amount in Sample [nmol]	Gd Amount per Cell [fmol/cell]
0	< 0.001	< 0.001	0.11	0.02
0.22	1.24	0.21	1.42	0.24
0.44	2.3	0.38	2.47	0.41
0.89	5.49	0.92	2.84	0.47
1.79	6.54	1.09	4.39	0.73

Table 2 ICP-AES analysis of cells in order to quantify the amount intracellular Gd 9 days after labeling.

Part 2 – Experiments with Embryonic Stem Cells

Experiment 5 – Differentiation of ES Cells to Neurons

As described, ES cells were differentiated into neurons. Morphologic evaluation as well as X-gal staining was performed to show successful differentiation into neurons (Figure 23). Note how the undifferentiated ES cells in the middle do not express *lacZ* and as such do not stain while the differentiating early neurons express *lacZ* and stain with X-gal.

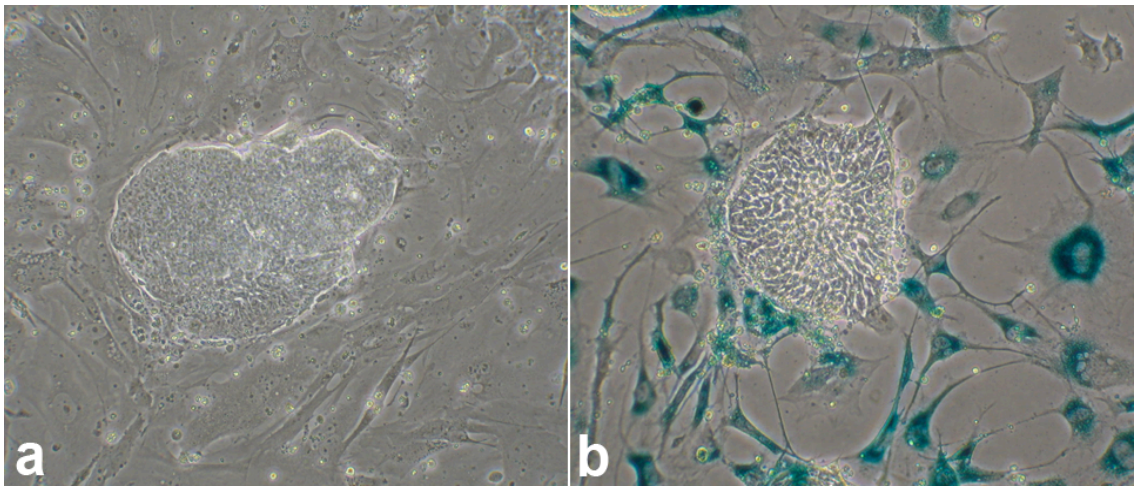

Figure 23 Light microscopy pictures of a colony of undifferentiated ES cells (center) surrounded by differentiating early neuronal cells without (a) and with (b) X-gal staining.

Given the dynamic nature of the differentiation process, X-gal stains were performed at multiple time points to find out when optimal numbers of differentiated, *lacZ*-producing cells were available. The same cell culture in various stages of the differentiation process can be seen in (Figure 24). As the cells grow non-adherently in three dimensions, the light microscopy pictures are slightly blurred.

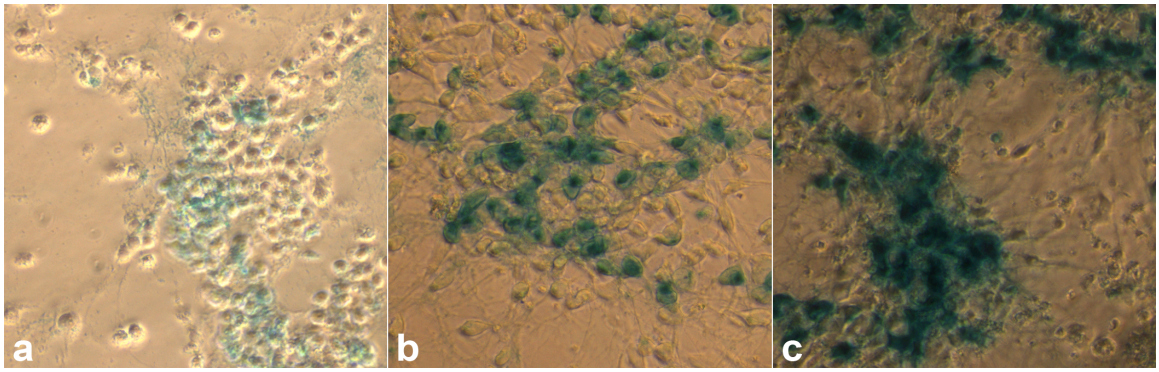

Figure 24 Light microscopy of X-gal stained differentiating ES cells on three consecutive days (a-c) in the differentiation process.

Experiment 6 – Detecting ES cell differentiation via MR scanning with EgadMe

Once ES cells were differentiated, they were labeled with EgadMe and compared with undifferentiated, labeled ES cells.

MR Imaging

SE images at varying TR/TE times can be seen in Figure 25. Labeled differentiated, β-galactosidase positive cells behaved quite contrary to our expectations. In the T_1-weighted 15/500 image the undifferentiated β-galactosidase negative cells displayed higher signal intensity when compared to the differentiated β-galactosidase positive cells. This speaks for a lack of T_1 effect of the contrast agent. On T_2-weighted images, the differentiated β-galactosidase positive cells displayed lower signal intensity, speaking for a T_2 effect of the contrast agent.

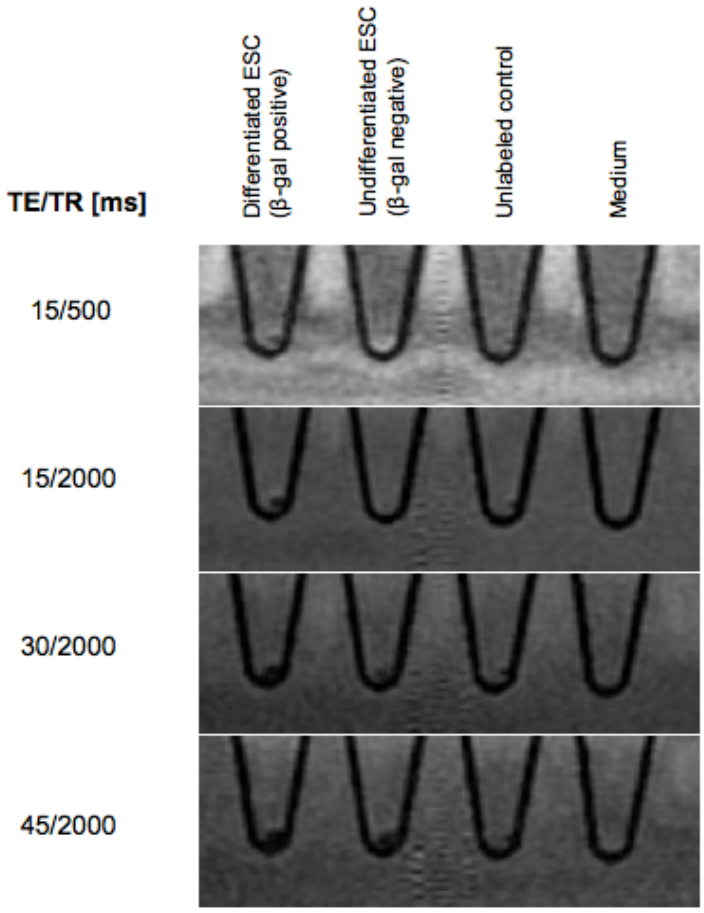

Figure 25 SE images at varying TE/TR of 1.5 x 10^7 β-galactosidase positive, differentiated and β-galactosidase negative, undifferentiated ES cells (both labeled with EgadMe) compared to unlabeled control and medium.

Discussion

In the scope of this thesis, we were able to show that the novel intelligent contrast agent EgadMe can be used as a marker of stem cell differentiation in non-invasive MR imaging. As the *lacZ* gene is used extensively in the field of molecular biology we believe that the future uses of EgadMe are promising.

EgadMe is internalized into cells when the transfection agent lipofectin is used. Lipofectin is typically used in the field of DNA transfection [14], however it has been found extremely useful with various other MR contrast agents such as gadolinium-based agents (Gadophrin-2, Gd-DTPA) and iron-based agents (ferumoxides, ferucarbotran) [17, 18, 21, 83]. The internalization of EgadMe into the cell likely involves fusion of EgadMe-lipofectin complexes with the cell membrane with subsequent delivery of the contrast agent into the cytosol [27]. Once in the cytosol, the contrast agent can interact with β-galactosidase. The labeling efficiencies we noticed were poor at less than 1‰ for every incubation concentration investigated (0.22 – 1.79 μmol/ml). This is in stark contrast to labeling efficiencies with similar Gd-based contrast agents. For example, Rudelius et al displayed efficiencies of up to 50% with embryonic and neuronal stem cells labeled with Gd-DTPA and lipofectine [83]. The ICP-AES measurements used to calculate labeling efficiency were performed 9 days after labeling, so there is a dilution effect where some contrast agent was lost to dividing cells. However cell growth in these 9 days was in the order of 2 passages. Thus, while dilution is one reason for the low amount of Gd intracellularly, it cannot account for the poor uptake of EgadeMe. While even the small amount of EgadMe that was internalized displayed both qualitative and quantitative effects in MR scanning, more efficient ways of mediating EgadMe uptake would be favorable.

Such more efficient transfection methods may include use of alternative transfection agents or use of different transfection methods altogether. Similar liposomal transfection can be achieved by using substances that are related to lipofectine but have shown to be more effective at conventional nucleic acid transfection [41]. Examples of such agents are Lipofectamine, Lipofectamine 2000

(both Invitrogen) or GenePORTER (Gene Therapy Systems). While in the setting of Gd-based contrast similar transfection efficiencies were achieved using lipofectine and Lipofectamine with ES and neuronal stem cells [83], it may be possible that more efficient results can be achieved with EgadMe and different transfection agent. Other transfection methods may be better suited to incorporate EgadMe into the stem cell. Electroporation is a method where the cell membrane is disrupted via electrical current for a short time in order to allow extracellular material to move inside the cell [17, 95]. This method allows for almost instant labeling with various types of contrast agents. However, there is conflicting data regarding cell viability and differentiation capacity of cells treated by electroporation with some groups allowing cells to recover for 24 hours before using them for further experiments [17]. Nevertheless, the ability to incorporate various types of contrast agent inside a cell is enticing and may allow for EgadMe to be internalized more efficiently than we were able to show.

We found that when higher concentrations of EgadMe were used (0.89 and 1.79 μmol/ml) cell clumps formed towards the end of the incubation process that were difficult to dissolve. After repeated washing with PBS we were able to dissolve the complexes and count individual cells in the cell counting chamber, however the cells labeled at the higher concentrations of EgadMe remained "sticky." As the ratio of lipofectin to EgadMe remained constant with increasing incubation concentrations of EgadMe, one possible explanation is that the cell uptake mechanisms were not efficient enough to keep up with the increased supply of the EgadMe-lipofectin complex. The contrast agent that was not internalized remained on the cell wall and caused cell-cell interaction that caused cell clumping. The amount of cell clumping was subjectively more pronounced with β-galactosidase positive cells. As it is well-known that previously transfected cell lines are more difficult to transfect again [17], this finding corroborates with our explanation. However, we are aware that without further detailed study, the exact mechanism of cell clumping can only be guessed. It is important though to keep this in mind as it has been shown that cell to cell contact is required for both stem cell proliferation as well as stem cell differentiation [28, 43].

The signal characteristics of EgadMe were both qualitatively and quantitatively measured in its inactive, uncleaved and its active, cleaved state.

However, if one compares our results with the publication where the smart contrast agent was originally introduced (Figure 6) one notices a much more pronounced effect in the original publication [66]. Moats et al introduced the actual enzyme β-galactosidase into solution with Egad (the predecessor of EgadMe) and incubated the solution for 7 days in order to allow for proper cleavage of the galactose ring. This compares with incubation times from 1 hour to 18 hours that were used for the Xgal staining. We utilized incubation times ranging from 4 to 12 hours and allowed cells 12 hours after labeling in order to cleave the galactose ring (Experiment 4). Such times were ample for Xgal staining but perhaps not long enough for cleavage of EgadMe. After 7 days of incubation with pure β-galactosidase enzyme, Moats et al found that more than 95% of the contrast agent had been cleaved [66]. We were unfortunately unable to determine the ration of uncleaved to cleaved EgadMe found within the cells after scanning. Given the fact that probably not all of the liposomally transfected EgadMe was visible to cytosolic β-galactosidase (i.e. some contrast was still inside micelles) and the extremely long metabolisation times noted by Moats et al, we feel it is likely that not all of the EgadMe was activated. This can explain the somewhat less pronounced contrast effect as expected.

Long-term labeling with EgadMe (Experiment 4) for a total of 9 days showed no detectable signal differences between unlabeled and labeled SVZ cells at varying EgadMe concentrations. ICP-AES did in fact show differences in intracellular Gd content, however the amounts were too low to be depicted on MR imaging. In different cell lines, single cell amounts of Gd in the range of 1 fmol per cell have been found to be sufficient for some change in MR signal (GadofluorineM in monocytes), while in other lines 10 to 100 times the Gd amount is required (Gd-DTPA in hematopoietic progenitor cells) [20, 38]. For SVZ cells we therefore conclude that more than 1 fmol per cell of Gd of EgadMe is required to generate visible changes in signal.

A small amount of Gd was detected in the control sample of β-galactosidase positive SVZ cells. We attribute this to artifacts in the ICP-AES process although some level of cross-contamination during long-term cell culturing cannot be excluded. However, the small amount of Gd found was unlikely to have an effect on signal or viability.

Unlabeled β-galactosidase positive and negative SVZ cells scanned at Day 0 and Day 9 displayed quite different T_1 relaxation times. These control cells were expected to display equal T_1 times throughout the entire process as they were not labeled with any contrast. A possible explanation is a changing composition of the intracellular space over time. It is well known that compartmentalized water shows different signal characteristics compared to free water [62]. Thus, the exact morphology and the distribution of intracellular water can affect MR signal characteristics of a cell. Although no major changes were seen in light microscopy of SVZ cells during the 9 days of long-term culture, this explanation remains a possibility why unequal T_1 relaxation times were measured.

Scanning of the differentiated and undifferentiated ES cells (Experiment 6) delivered somewhat surprising results. The EgadMe internalized by the differentiated, β-galactosidase positive ES cells displayed a predominant T_2 contrast effect in lieu of the T_1 effect that was expected. At high concentrations, the ability of Gd to interact with water molecules is limited and thus the Gd causes local field inhomogeneities leading to a T_2 effect [11, 86]. A high concentration of intracellular EgadMe may explain the predominant T_2 effect seen. However, this is in contrast to the behavior seen with SVZ cells where the cell uptake of Gd was ample, but by no means efficient enough to obtain the high concentrations in order to see a predominantly T_2 effect of EgadMe. Unfortunately, we were unable to perform ICP-AES analysis to quantify the exact amount of intracellular Gd.

While scanning differentiated and undifferentiated ES cells, the limitations of metabolisation time and cell uptake already described for SVZ cells also hold true. In addition, ES cells display the added limitation of differentiation state. We used doublecortin, a microtubule-associated protein characteristic of neuroblasts, as our promoter for *lacZ* expression [65]. As such, in the differentiation process between an ES cell and a neuron, the expression of doublecortin is not constant and is never 100% of an entire cell population (Figure 3). In the differentiating population, one always finds cells that are in the beginning (ES cell, neuronal stem cell) and cells that are at the end of the differentiation process (immature neuron, mature neuron). As can be seen in Figure 24, the amount of *lacZ* expressing cells steadily increased with

time. However, we were unable to wait until all cells stained blue as then a portion of the cells would become mature neurons and stop expressing doublecortin and as such would stop expressing *lacZ*. Therefore, only a large subset of "differentiated" ES cells expressed *lacZ* and was able to cleave EgadMe. This undoubtedly had the effect of not all EgadMe being activated before scanning. In comparison, the SVZ cells used were treated with a viral vector and subsequent elimination of non-infected cells via the neomycin resistance gene. As such, almost 100% of transfected SVZ cells were β-galactosidase positive and were able to activate EgadMe by cleavage.

We were also unfortunately unable to perform additional studies on ES cells because of the extreme difficulty and cost related to ES cell culture. The rationale of utilizing the SVZ cell line as a testing line before performing experiments on ES cells was to circumvent these limitations, however, as shown by the differences in cell uptake characteristics and *lacZ* expression between SVZ and ES cells, this was only partially true. In order to truly optimize EgadMe labeling and imaging for the function of visualizing ES differentiation, it is necessary that these experiments be completed in ES cells.

In conclusion, we have shown EgadMe to be a promising novel smart contrast agent. Our experiments with SVZ cells showed both qualitative and quantitative changes between β-galactosidase positive and negative cells on MR scanning after labeling with EgadMe. Experiments with ES cells were hampered by reasons previously described, although a promising, T_2 contrast effect was seen. Further studies are undoubtedly needed, however the goal of visualizing stem cell differentiation using a non-invasive method is surely one step closer to realization.

Summary

Stem cell therapy is a promising novel therapeutic approach for a variety of diseases. Many therapy strategies involve implantation of exogenous stem cells into the body, however, determining what happens to these stem cells after application is difficult. Magnetic resonance imaging is a non-invasive imaging method that does not utilize ionizing radiation and has the potential to aid in answering this question. Previously, work has been completed to image homing of cells inside the body. These imaging methods are able to depict where cells go after application, however, they are unable to assess whether or not stem cells differentiate into target tissue or not.

In the scope of this MD thesis, EgadMe, a novel gadolinium based T_1 enhancing intelligent contrast agent for MR imaging, was used to depict gene expression and stem cell differentiation. EgadMe has the property of being activated by β-galactosidase, a widely used reporter gene. Experiments were done with mouse subventricular zone (SVZ) adult neuronal stem cells modified to express β-galactosidase. We were able to show that β-galactosidase positive SVZ cells result in increased signal when compared to β-galactosidase negative controls. Further experiments were conducted with mouse embryonal stem cells modified to the effect where they produced β-galactosidase upon differentiation into neurons. Upon imaging, differentiated embryonal stem cells displayed a prominent T_2 signal decrease compared to undifferentiated controls.

We were able to show that the novel, intelligent contrast agent EgadMe has the potential to depict gene expression and stem cell differentiation non-invasively. This will allow for future applications of non-invasive, real-time depiction of gene expression and stem cell differentiation.

References

1. Alauddin, M.M., A.Y. Louie, A. Shahinian, T.J. Meade, and P.S. Conti, *Receptor mediated uptake of a radiolabeled contrast agent sensitive to beta-galactosidase activity.* Nucl Med Biol, 2003. **30**(3): p. 261-265.
2. Alvarez-Buylla, A., B. Seri, and F. Doetsch, *Identification of neural stem cells in the adult vertebrate brain.* Brain Res Bull, 2002. **57**(6): p. 751-758.
3. Anderson, S.A., J. Glod, A.S. Arbab, M. Noel, P. Ashari, H.A. Fine, and J.A. Frank, *Noninvasive MR imaging of magnetically labeled stem cells to directly identify neovasculature in a glioma model.* Blood, 2005. **105**(1): p. 420-425.
4. Arbab, A.S., G.T. Yocum, H. Kalish, E.K. Jordan, S.A. Anderson, A.Y. Khakoo, E.J. Read, and J.A. Frank, *Efficient magnetic cell labeling with protamine sulfate complexed to ferumoxides for cellular MRI.* Blood, 2004. **104**(4): p. 1217-1223.
5. Artemov, D., N. Mori, R. Ravi, and Z.M. Bhujwalla, *Magnetic resonance molecular imaging of the HER-2/neu receptor.* Cancer Res, 2003. **63**(11): p. 2723-2727.
6. Askenasy, N., E.S. Yolcu, H. Shirwan, J. Stein, I. Yaniv, and D.L. Farkas, *Characterization of adhesion and viability of early seeding hematopoietic cells in the host bone marrow in vivo and in situ.* Exp Hematol, 2003. **31**(12): p. 1292-1300.
7. Beltrami, A.P., K. Urbanek, J. Kajstura, S.M. Yan, N. Finato, R. Bussani, B. Nadal-Ginard, F. Silvestri, A. Leri, C.A. Beltrami, and P. Anversa, *Evidence that human cardiac myocytes divide after myocardial infarction.* N Engl J Med, 2001. **344**(23): p. 1750-1757.
8. Bhorade, R., R. Weissleder, T. Nakakoshi, A. Moore, and C.H. Tung, *Macrocyclic chelators with paramagnetic cations are internalized into mammalian cells via a HIV-tat derived membrane translocation peptide.* Bioconjug Chem, 2000. **11**(3): p. 301-305.
9. Bignami, A., L.F. Eng, D. Dahl, and C.T. Uyeda, *Localization of the glial fibrillary acidic protein in astrocytes by immunofluorescence.* Brain Res, 1972. **43**(2): p. 429-435.
10. Buhling, F., A. Fengler, W. Brandt, T. Welte, S. Ansorge, and D.K. Nagler, *Review: novel cysteine proteases of the papain family.* Adv Exp Med Biol, 2000. **477**: p. 241-254.
11. Burstein, D., A. Williams, C. McKenzie, K. Woertler, and E.J. Rummeny, *Potential for misinterpretation of combined T1- and T2-weighted contrast-enhanced MR imaging of cartilage.* Radiology, 2004. **233**(2): p. 619-620; author reply 621-612.
12. Cavagna, F.M., F. Maggioni, P.M. Castelli, M. Dapra, L.G. Imperatori, V. Lorusso, and B.G. Jenkins, *Gadolinium chelates with weak binding to serum proteins. A new class of high-efficiency, general purpose contrast agents for magnetic resonance imaging.* Invest Radiol, 1997. **32**(12): p. 780-796.
13. Cepko, C., E. Ryder, D.M. Fekete, and S. Bruhn. *Detection of β-galactosidase and alkaline phosphatase in tissue*. Available from: http://genetics.med.harvard.edu/~cepko/protocol/xgalplap-stain.htm.

14. Coonrod, A., F.Q. Li, and M. Horwitz, *On the mechanism of DNA transfection: efficient gene transfer without viruses.* Gene Ther, 1997. **4**(12): p. 1313-1321.
15. Corbo, J.C., T.A. Deuel, J.M. Long, P. LaPorte, E. Tsai, A. Wynshaw-Boris, and C.A. Walsh, *Doublecortin is required in mice for lamination of the hippocampus but not the neocortex.* J Neurosci, 2002. **22**(17): p. 7548-7557.
16. Crich, S.G., L. Biancone, V. Cantaluppi, D. Duo, G. Esposito, S. Russo, G. Camussi, and S. Aime, *Improved route for the visualization of stem cells labeled with a Gd-/Eu-chelate as dual (MRI and fluorescence) agent.* Magn Reson Med, 2004. **51**(5): p. 938-944.
17. Daldrup-Link, H.E., R. Meier, M. Rudelius, G. Piontek, M. Piert, S. Metz, M. Settles, C. Uherek, W. Wels, J. Schlegel, and E.J. Rummeny, *In vivo tracking of genetically engineered, anti-HER2/neu directed natural killer cells to HER2/neu positive mammary tumors with magnetic resonance imaging.* Eur Radiol, 2005. **15**(1): p. 4-13.
18. Daldrup-Link, H.E., M. Rudelius, S. Metz, G. Piontek, B. Pichler, M. Settles, U. Heinzmann, J. Schlegel, R.A. Oostendorp, and E.J. Rummeny, *Cell tracking with gadophrin-2: a bifunctional contrast agent for MR imaging, optical imaging, and fluorescence microscopy.* Eur J Nucl Med Mol Imaging, 2004. **31**(9): p. 1312-1321.
19. Daldrup-Link, H.E., M. Rudelius, R.A. Oostendorp, V.R. Jacobs, G.H. Simon, C. Gooding, and E.J. Rummeny, *Comparison of iron oxide labeling properties of hematopoietic progenitor cells from umbilical cord blood and from peripheral blood for subsequent in vivo tracking in a xenotransplant mouse model XXX.* Acad Radiol, 2005. **12**(4): p. 502-510.
20. Daldrup-Link, H.E., M. Rudelius, R.A. Oostendorp, M. Settles, G. Piontek, S. Metz, H. Rosenbrock, U. Keller, U. Heinzmann, E.J. Rummeny, J. Schlegel, and T.M. Link, *Targeting of hematopoietic progenitor cells with MR contrast agents.* Radiology, 2003. **228**(3): p. 760-767.
21. Daldrup-Link, H.E., M. Rudelius, G. Piontek, S. Metz, R. Brauer, G. Debus, C. Corot, J. Schlegel, T.M. Link, C. Peschel, E.J. Rummeny, and R.A. Oostendorp, *Migration of iron oxide-labeled human hematopoietic progenitor cells in a mouse model: in vivo monitoring with 1.5-T MR imaging equipment.* Radiology, 2005. **234**(1): p. 197-205.
22. Deng, C.X., A. Wynshaw-Boris, M.M. Shen, C. Daugherty, D.M. Ornitz, and P. Leder, *Murine FGFR-1 is required for early postimplantation growth and axial organization.* Genes Dev, 1994. **8**(24): p. 3045-3057.
23. Dennis, K., M. Uittenbogaard, A. Chiaramello, and S.A. Moody, *Cloning and characterization of the 5'-flanking region of the rat neuron-specific Class III beta-tubulin gene.* Gene, 2002. **294**(1-2): p. 269-277.
24. Ding, W., J. Bai, J. Zhang, Y. Chen, L. Cao, Y. He, L. Shen, F. Wang, and J. Tian, *In vivo tracking of implanted stem cells using radio-labeled transferrin scintigraphy.* Nucl Med Biol, 2004. **31**(6): p. 719-725.
25. Emsley, J.G., B.D. Mitchell, G. Kempermann, and J.D. Macklis, *Adult neurogenesis and repair of the adult CNS with neural progenitors, precursors, and stem cells.* Prog Neurobiol, 2005. **75**(5): p. 321-341.
26. Evans, M.J. and M.H. Kaufman, *Establishment in culture of pluripotential cells from mouse embryos.* Nature, 1981. **292**(5819): p. 154-156.

27. Felgner, P.L., T.R. Gadek, M. Holm, R. Roman, H.W. Chan, M. Wenz, J.P. Northrop, G.M. Ringold, and M. Danielsen, *Lipofection: a highly efficient, lipid-mediated DNA-transfection procedure.* Proc Natl Acad Sci U S A, 1987. **84**(21): p. 7413-7417.
28. Fox, V., P.J. Gokhale, J.R. Walsh, M. Matin, M. Jones, and P.W. Andrews, *Cell-cell signaling through NOTCH regulates human embryonic stem cell proliferation.* Stem Cells, 2008. **26**(3): p. 715-723.
29. Frangioni, J.V. and R.J. Hajjar, *In vivo tracking of stem cells for clinical trials in cardiovascular disease.* Circulation, 2004. **110**(21): p. 3378-3383.
30. Frank, J.A., B.R. Miller, A.S. Arbab, H.A. Zywicke, E.K. Jordan, B.K. Lewis, L.H. Bryant, Jr., and J.W. Bulte, *Clinically applicable labeling of mammalian and stem cells by combining superparamagnetic iron oxides and transfection agents.* Radiology, 2003. **228**(2): p. 480-487.
31. Freed, C.R., P.E. Greene, R.E. Breeze, W.Y. Tsai, W. DuMouchel, R. Kao, S. Dillon, H. Winfield, S. Culver, J.Q. Trojanowski, D. Eidelberg, and S. Fahn, *Transplantation of embryonic dopamine neurons for severe Parkinson's disease.* N Engl J Med, 2001. **344**(10): p. 710-719.
32. Freshney, R., *Culture of Animal Cells: A Manual of Basic Technique*. 1987, New York: Alan R. Liss, Inc.
33. Gao, X. and S. Nie, *Quantum dot-encoded mesoporous beads with high brightness and uniformity: rapid readout using flow cytometry.* Anal Chem, 2004. **76**(8): p. 2406-2410.
34. Genove, G., U. DeMarco, H. Xu, W.F. Goins, and E.T. Ahrens, *A new transgene reporter for in vivo magnetic resonance imaging.* Nat Med, 2005. **11**(4): p. 450-454.
35. Good, N.E., G.D. Winget, W. Winter, T.N. Connolly, S. Izawa, and R.M. Singh, *Hydrogen ion buffers for biological research.* Biochemistry, 1966. **5**(2): p. 467-477.
36. Haider, H. and M. Ashraf, *Bone marrow stem cell transplantation for cardiac repair.* Am J Physiol Heart Circ Physiol, 2005. **288**(6): p. H2557-2567.
37. Health, N.I.o., *Stem Cells - Scientific Progress and Future Research Directions*. 2001.
38. Henning, T.D., O. Saborowski, D. Golovko, S. Boddington, J.S. Bauer, Y. Fu, R. Meier, H. Pietsch, B. Sennino, D.M. McDonald, and H.E. Daldrup-Link, *Cell labeling with the positive MR contrast agent Gadofluorine M.* Eur Radiol, 2007. **17**(5): p. 1226-1234.
39. Hoehn, M., E. Kustermann, J. Blunk, D. Wiedermann, T. Trapp, S. Wecker, M. Focking, H. Arnold, J. Hescheler, B.K. Fleischmann, W. Schwindt, and C. Buhrle, *Monitoring of implanted stem cell migration in vivo: a highly resolved in vivo magnetic resonance imaging investigation of experimental stroke in rat.* Proc Natl Acad Sci U S A, 2002. **99**(25): p. 16267-16272.
40. Holt, S.J. and P.W. Sadler, *Studies in enzyme cytochemistry. III. Relationships between solubility, molecular association and structure in indigoid dyes.* Proc R Soc Lond B Biol Sci, 1958. **148**(933): p. 495-505.
41. Iversen, N., B. Birkenes, K. Torsdalen, and S. Djurovic, *Electroporation by nucleofector is the best nonviral transfection technique in human endothelial and smooth muscle cells.* Genet Vaccines Ther, 2005. **3**(1): p. 2.
42. Jaffer, F.A. and R. Weissleder, *Molecular imaging in the clinical arena.* Jama, 2005. **293**(7): p. 855-862.

43. Jensen, C.G., C.A. Poole, S.R. McGlashan, M. Marko, Z.I. Issa, K.V. Vujcich, and S.S. Bowser, *Ultrastructural, tomographic and confocal imaging of the chondrocyte primary cilium in situ.* Cell Biol Int, 2004. **28**(2): p. 101-110.
44. Jiang, W., E. Papa, H. Fischer, S. Mardyani, and W.C. Chan, *Semiconductor quantum dots as contrast agents for whole animal imaging.* Trends Biotechnol, 2004. **22**(12): p. 607-609.
45. Jiang, Y., B.N. Jahagirdar, R.L. Reinhardt, R.E. Schwartz, C.D. Keene, X.R. Ortiz-Gonzalez, M. Reyes, T. Lenvik, T. Lund, M. Blackstad, J. Du, S. Aldrich, A. Lisberg, W.C. Low, D.A. Largaespada, and C.M. Verfaillie, *Pluripotency of mesenchymal stem cells derived from adult marrow.* Nature, 2002. **418**(6893): p. 41-49.
46. Josephson, L., M.J. Perez, and R. Weissleder, *Magnetic Nanosensors for the Detection of Oligonucleotide Sequences.* Angew Chem Int Ed, 2001. **40**(17): p. 3204-3206.
47. Kerr, D.A., J. Llado, M.J. Shamblott, N.J. Maragakis, D.N. Irani, T.O. Crawford, C. Krishnan, S. Dike, J.D. Gearhart, and J.D. Rothstein, *Human embryonic germ cell derivatives facilitate motor recovery of rats with diffuse motor neuron injury.* J Neurosci, 2003. **23**(12): p. 5131-5140.
48. Kimelberg, H.K., *The problem of astrocyte identity.* Neurochem Int, 2004. **45**(2-3): p. 191-202.
49. Kleppner, S.R., K.A. Robinson, J.Q. Trojanowski, and V.M. Lee, *Transplanted human neurons derived from a teratocarcinoma cell line (NTera-2) mature, integrate, and survive for over 1 year in the nude mouse brain.* J Comp Neurol, 1995. **357**(4): p. 618-632.
50. Klug, M.G., M.H. Soonpaa, G.Y. Koh, and L.J. Field, *Genetically selected cardiomyocytes from differentiating embronic stem cells form stable intracardiac grafts.* J Clin Invest, 1996. **98**(1): p. 216-224.
51. Kobayashi, H. and M.W. Brechbiel, *Dendrimer-based macromolecular MRI contrast agents: characteristics and application.* Mol Imaging, 2003. **2**(1): p. 1-10.
52. Kondziolka, D., L. Wechsler, S. Goldstein, C. Meltzer, K.R. Thulborn, J. Gebel, P. Jannetta, S. DeCesare, E.M. Elder, M. McGrogan, M.A. Reitman, and L. Bynum, *Transplantation of cultured human neuronal cells for patients with stroke.* Neurology, 2000. **55**(4): p. 565-569.
53. Kos, C.H., *Cre/loxP system for generating tissue-specific knockout mouse models.* Nutr Rev, 2004. **62**(6 Pt 1): p. 243-246.
54. Lakshmipathy, U. and C. Verfaillie, *Stem cell plasticity.* Blood Rev, 2005. **19**(1): p. 29-38.
55. Laxman, B., D.E. Hall, M.S. Bhojani, D.A. Hamstra, T.L. Chenevert, B.D. Ross, and A. Rehemtulla, *Noninvasive real-time imaging of apoptosis.* Proc Natl Acad Sci U S A, 2002. **99**(26): p. 16551-16555.
56. Lepore, A.C. and I. Fischer, *Lineage-restricted neural precursors survive, migrate, and differentiate following transplantation into the injured adult spinal cord.* Exp Neurol, 2005. **194**(1): p. 230-242.
57. Li, W.H., G. Parigi, M. Fragai, C. Luchinat, and T.J. Meade, *Mechanistic studies of a calcium-dependent MRI contrast agent.* Inorg Chem, 2002. **41**(15): p. 4018-4024.
58. Lindvall, O. and Z. Kokaia, *Recovery and rehabilitation in stroke: stem cells.* Stroke, 2004. **35**(11 Suppl 1): p. 2691-2694.

59. Liu, F. and L. Huang, *Development of non-viral vectors for systemic gene delivery.* J Control Release, 2002. **78**(1-3): p. 259-266.
60. Long, X., M. Olszewski, W. Huang, and M. Kletzel, *Neural cell differentiation in vitro from adult human bone marrow mesenchymal stem cells.* Stem Cells Dev, 2005. **14**(1): p. 65-69.
61. Louie, A.Y., M.M. Huber, E.T. Ahrens, U. Rothbacher, R. Moats, R.E. Jacobs, S.E. Fraser, and T.J. Meade, *In vivo visualization of gene expression using magnetic resonance imaging.* Nat Biotechnol, 2000. **18**(3): p. 321-325.
62. Matsumae, M., S. Oi, H. Watanabe, K. Okamoto, Y. Suzuki, K. Sato, H. Atsumi, T. Goto, and R. Tsugane, *Distribution of intracellular and extracellular water molecules in developing rat's midbrain: comparison with fraction of multicomponent T(2) relaxation time and morphological findings from electron microscopic imaging.* Childs Nerv Syst, 2003. **19**(2): p. 91-95.
63. Meade, T.J., A.K. Taylor, and S.R. Bull, *New magnetic resonance contrast agents as biochemical reporters.* Curr Opin Neurobiol, 2003. **13**(5): p. 597-602.
64. Medicine, U.S.N.L.o. *DailyMed Current Medication Information*. 2006 [cited 2007; Available from: http://dailymed.nlm.nih.gov/dailymed/drugInfo.cfm?id=671.
65. Mignone, J.L., V. Kukekov, A.S. Chiang, D. Steindler, and G. Enikolopov, *Neural stem and progenitor cells in nestin-GFP transgenic mice.* J Comp Neurol, 2004. **469**(3): p. 311-324.
66. Moats, R., S.E. Fraser, and T.J. Meade, *A "Smart" Magnetic Resonance Imaging Agent That Reports on Specific Enzymatic Activity.* Angew Chem Int Ed, 1997. **36**(7): p. 725-728.
67. Modo, M., D. Cash, K. Mellodew, S.C. Williams, S.E. Fraser, T.J. Meade, J. Price, and H. Hodges, *Tracking transplanted stem cell migration using bifunctional, contrast agent-enhanced, magnetic resonance imaging.* Neuroimage, 2002. **17**(2): p. 803-811.
68. Mügge, C. *NMR Spectroscopy Website*. [cited 2005 15 August]; Available from: http://www2.hu-berlin.de/chemie/nmr/research-subjects/research-kontrastmittel-de.htm.
69. Murray, R.W., D.J. Miller, and K.A. Kryc (2000) *Analysis of Major and Trace Elements in Rocks, Sediments, and Interstitial Waters by Inductively Coupled Plasma-Atomic Emission Spectrometry (ICP-AES)*. ODP Tech. Note **29**.
70. Nichols, J., E.P. Evans, and A.G. Smith, *Establishment of germ-line-competent embryonic stem (ES) cells using differentiation inhibiting activity.* Development, 1990. **110**(4): p. 1341-1348.
71. Nunes, M.C., N.S. Roy, H.M. Keyoung, R.R. Goodman, G. McKhann, 2nd, L. Jiang, J. Kang, M. Nedergaard, and S.A. Goldman, *Identification and isolation of multipotential neural progenitor cells from the subcortical white matter of the adult human brain.* Nat Med, 2003. **9**(4): p. 439-447.
72. Olanow, C.W., C.G. Goetz, J.H. Kordower, A.J. Stoessl, V. Sossi, M.F. Brin, K.M. Shannon, G.M. Nauert, D.P. Perl, J. Godbold, and T.B. Freeman, *A double-blind controlled trial of bilateral fetal nigral transplantation in Parkinson's disease.* Ann Neurol, 2003. **54**(3): p. 403-414.
73. Oliver, T.G. and R.J. Wechsler-Reya, *Getting at the root and stem of brain tumors.* Neuron, 2004. **42**(6): p. 885-888.

74. Pan, Y., X. Chen, S. Wang, S. Yang, X. Bai, X. Chi, K. Li, B. Liu, and L. Li, *In vitro neuronal differentiation of cultured human embryonic germ cells.* Biochem Biophys Res Commun, 2005. **327**(2): p. 548-556.
75. Park, K.I., *Transplantation of neural stem cells: cellular & gene therapy for hypoxic-ischemic brain injury.* Yonsei Med J, 2000. **41**(6): p. 825-835.
76. Perez, J.M., L. Josephson, and R. Weissleder, *Use of magnetic nanoparticles as nanosensors to probe for molecular interactions.* Chembiochem, 2004. **5**(3): p. 261-264.
77. Persigehl, T., W. Heindel, and C. Bremer, *MR and optical approaches to molecular imaging.* Abdom Imaging, 2005. **30**(3): p. 342-354.
78. Picard-Riera, N., B. Nait-Oumesmar, and A. Baron-Van Evercooren, *Endogenous adult neural stem cells: limits and potential to repair the injured central nervous system.* J Neurosci Res, 2004. **76**(2): p. 223-231.
79. Reubinoff, B.E., P. Itsykson, T. Turetsky, M.F. Pera, E. Reinhartz, A. Itzik, and T. Ben-Hur, *Neural progenitors from human embryonic stem cells.* Nat Biotechnol, 2001. **19**(12): p. 1134-1140.
80. Rinck, P.A., *Magnetic Resonance in Medicine*. 3rd Edition ed. 1993: Blackwell Scientific Publications.
81. Rohrer, M., H. Bauer, J. Mintorovitch, M. Requardt, and H.J. Weinmann, *Comparison of magnetic properties of MRI contrast media solutions at different magnetic field strengths.* Invest Radiol, 2005. **40**(11): p. 715-724.
82. Roybon, L., N.S. Christophersen, P. Brundin, and J.Y. Li, *Stem cell therapy for Parkinson's disease: where do we stand?* Cell Tissue Res, 2004. **318**(1): p. 261-273.
83. Rudelius, M., H.E. Daldrup-Link, U. Heinzmann, G. Piontek, M. Settles, T.M. Link, and J. Schlegel, *Highly efficient paramagnetic labelling of embryonic and neuronal stem cells.* Eur J Nucl Med Mol Imaging, 2003. **30**(7): p. 1038-1044.
84. Saporta, S., A.S. Makoui, A.E. Willing, M. Daadi, D.W. Cahill, and P.R. Sanberg, *Functional recovery after complete contusion injury to the spinal cord and transplantation of human neuroteratocarcinoma neurons in rats.* J Neurosurg, 2002. **97**(1 Suppl): p. 63-68.
85. Simon, G.H., J. von Vopelius-Feldt, M.F. Wendland, Y. Fu, G. Piontek, J. Schlegel, M.H. Chen, and H.E. Daldrup-Link, *MRI of arthritis: comparison of ultrasmall superparamagnetic iron oxide vs. Gd-DTPA.* J Magn Reson Imaging, 2006. **23**(5): p. 720-727.
86. Smith, R.C. and R.C. Lange, *Understanding Magnetic Resonance Imaging*. 1998: CRC Press.
87. Soonpaa, M.H., G.Y. Koh, M.G. Klug, and L.J. Field, *Formation of nascent intercalated disks between grafted fetal cardiomyocytes and host myocardium.* Science, 1994. **264**(5155): p. 98-101.
88. Soria, B., E. Roche, G. Berna, T. Leon-Quinto, J.A. Reig, and F. Martin, *Insulin-secreting cells derived from embryonic stem cells normalize glycemia in streptozotocin-induced diabetic mice.* Diabetes, 2000. **49**(2): p. 157-162.
89. Soriano, P., *Generalized lacZ expression with the ROSA26 Cre reporter strain.* Nat Genet, 1999. **21**(1): p. 70-71.
90. Strauer, B.E., M. Brehm, T. Zeus, M. Kostering, A. Hernandez, R.V. Sorg, G. Kogler, and P. Wernet, *Repair of infarcted myocardium by autologous intracoronary mononuclear bone marrow cell transplantation in humans.* Circulation, 2002. **106**(15): p. 1913-1918.

91. Street, C.N., S. Sipione, L. Helms, T. Binette, R.V. Rajotte, R.C. Bleackley, and G.S. Korbutt, *Stem cell-based approaches to solving the problem of tissue supply for islet transplantation in type 1 diabetes.* Int J Biochem Cell Biol, 2004. **36**(4): p. 667-683.
92. Thomson, J.A., J. Itskovitz-Eldor, S.S. Shapiro, M.A. Waknitz, J.J. Swiergiel, V.S. Marshall, and J.M. Jones, *Embryonic stem cell lines derived from human blastocysts.* Science, 1998. **282**(5391): p. 1145-1147.
93. Tolar, J., M. Osborn, S. Bell, R. McElmurry, L. Xia, M. Riddle, A. Panoskaltsis-Mortari, Y. Jiang, R.S. McIvor, C.H. Contag, S.R. Yant, M.A. Kay, C.M. Verfaillie, and B.R. Blazar, *Real-time in vivo imaging of stem cells following transgenesis by transposition.* Mol Ther, 2005. **12**(1): p. 42-48.
94. Uchida, K., T. Momiyama, H. Okano, M. Yuzaki, A. Koizumi, Y. Mine, and T. Kawase, *Potential functional neural repair with grafted neural stem cells of early embryonic neuroepithelial origin.* Neurosci Res, 2005. **52**(3): p. 276-286.
95. Walczak, P., D.A. Kedziorek, A.A. Gilad, S. Lin, and J.W. Bulte, *Instant MR labeling of stem cells using magnetoelectroporation.* Magn Reson Med, 2005. **54**(4): p. 769-774.
96. Way, L.W. and G.M. Doherty, *Current Surgical Diagnosis and Treatment*. Vol. 11th Edition. 2003.
97. Weaver, J.C., *Electroporation: a general phenomenon for manipulating cells and tissues.* J Cell Biochem, 1993. **51**(4): p. 426-435.
98. Weinmann, H.J., W. Ebert, B. Misselwitz, and H. Schmitt-Willich, *Tissue-specific MR contrast agents.* Eur J Radiol, 2003. **46**(1): p. 33-44.
99. Weissleder, R., A. Moore, U. Mahmood, R. Bhorade, H. Benveniste, E.A. Chiocca, and J.P. Basilion, *In vivo magnetic resonance imaging of transgene expression.* Nat Med, 2000. **6**(3): p. 351-355.
100. Wu, X., H. Liu, J. Liu, K.N. Haley, J.A. Treadway, J.P. Larson, N. Ge, F. Peale, and M.P. Bruchez, *Immunofluorescent labeling of cancer marker Her2 and other cellular targets with semiconductor quantum dots.* Nat Biotechnol, 2003. **21**(1): p. 41-46.
101. Xu, H., X. Fan, J. Tang, G. Zhou, L. Yang, X. Wu, S. Liu, J. Qu, and H. Yang, *A modified method for generation of neural precursor cells from cultured mouse embryonic stem cells.* Brain Res Brain Res Protoc, 2005. **15**(1): p. 52-58.
102. Zambrowicz, B.P., A. Imamoto, S. Fiering, L.A. Herzenberg, W.G. Kerr, and P. Soriano, *Disruption of overlapping transcripts in the ROSA beta geo 26 gene trap strain leads to widespread expression of beta-galactosidase in mouse embryos and hematopoietic cells.* Proc Natl Acad Sci U S A, 1997. **94**(8): p. 3789-3794.